Immunity

Functional convergence of a germline-encoded neutralizing antibody response in rhesus macaques immunized with HCV envelope glycoproteins

Graphical Abstract

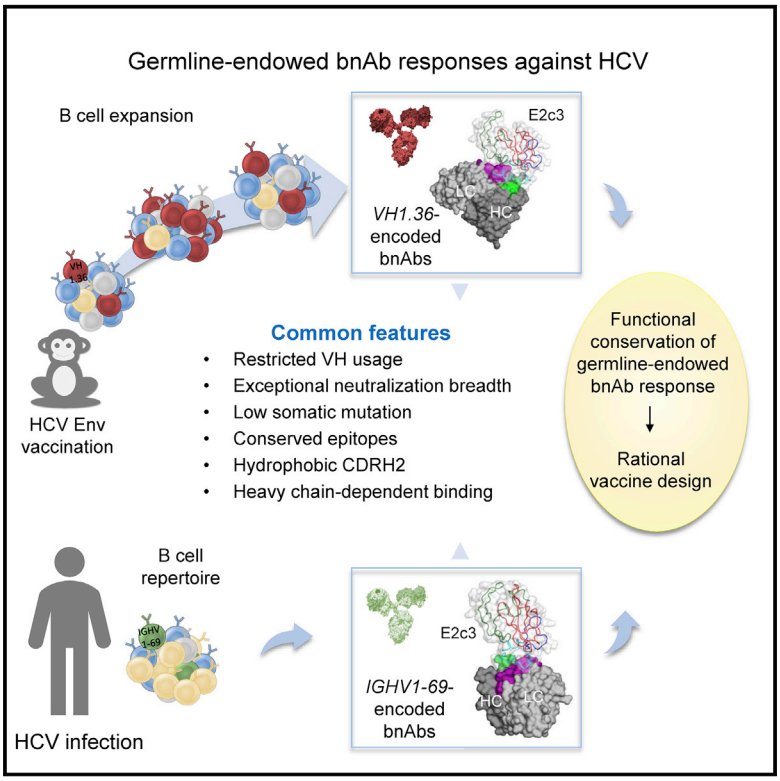

Highlights

- HCV Env immunization elicited a *VH1.36*-encoded bnAb response in rhesus macaques
- Macaque *VH1.36*- and human *IGHV1-69*-encoded bnAbs share common features
- Macaque bnAbs adopt different binding modes to recognize a flexible antigenic surface
- bnAbs mature functionally through rapid lineage development with few SHM

Authors

Fang Chen, Netanel Tzarum, Xiaohe Lin, ..., Ian A. Wilson, Jiang Zhu, Mansun Law

Correspondence

wilson@scripps.edu (I.A.W.), jiang@scripps.edu (J.Z.), mlaw@scripps.edu (M.L.)

In brief

The human *IGHV1-69* gene is preferentially utilized in broadly neutralizing antibody (bnAb) responses against HCV infection. Chen et al. discovered that HCV Env immunization of macaques elicited analogous *VH1.36* bnAbs on the functional and molecular level. Functional convergence of a corresponding germline-encoded bnAb response within primates has implications for HCV rational vaccine design and testing.

Chen et al., 2021, Immunity *54*, 1–16
April 13, 2021
https://doi.org/10.1016/j.immuni.2021.02.013

CellPress

Immunity

CellPress

Article

Functional convergence of a germline-encoded neutralizing antibody response in rhesus macaques immunized with HCV envelope glycoproteins

Fang Chen,[1,7] Netanel Tzarum,[2,7,8] Xiaohe Lin,[1] Erick Giang,[1] Rodrigo Velázquez-Moctezuma,[3] Elias H. Augestad,[3] Kenna Nagy,[1] Linling He,[1] Mayda Hernandez,[4] Mallorie E. Fouch,[4] Ariadna Grinyó,[4] Deborah Chavez,[5] Benjamin J. Doranz,[4] Jannick Prentoe,[3] Robyn L. Stanfield,[2] Robert Lanford,[5] Jens Bukh,[3] Ian A. Wilson,[2,6,*] Jiang Zhu,[1,2,*] and Mansun Law[1,9,*]

[1]Department of Immunology and Microbiology, The Scripps Research Institute, La Jolla, CA 92037, USA
[2]Department of Integrative Structural and Computational Biology, The Scripps Research Institute, La Jolla, CA 92037, USA
[3]Copenhagen Hepatitis C Program (CO-HEP), Department of Infectious Diseases, Hvidovre Hospital, and Department of Immunology and Microbiology, Faculty of Health and Medical Sciences, University of Copenhagen, Denmark
[4]Integral Molecular, Inc., Philadelphia, PA 19104, USA
[5]Southwest National Primate Research Center at Texas Biomedical Research Institute, San Antonio, TX 788227, USA
[6]Skaggs Institute for Chemical Biology, The Scripps Research Institute, La Jolla, CA 92037, USA
[7]These authors contributed equally
[8]Present address: Department of Biological Chemistry, Alexander Silberman Institute of Life Sciences, Faculty of Mathematics & Science, The Hebrew University of Jerusalem, Jerusalem 9190401, Israel
[9]Lead contact
*Correspondence: wilson@scripps.edu (I.A.W.), jiang@scripps.edu (J.Z.), mlaw@scripps.edu (M.L.)
https://doi.org/10.1016/j.immuni.2021.02.013

SUMMARY

Human *IGHV1-69*-encoded broadly neutralizing antibodies (bnAbs) that target the hepatitis C virus (HCV) envelope glycoprotein (Env) E2 are important for protection against HCV infection. An *IGHV1-69* ortholog gene, *VH1.36*, is preferentially used for bnAbs isolated from HCV Env-immunized rhesus macaques (RMs). Here, we studied the genetic, structural, and functional properties of *VH1.36*-encoded bnAbs generated by vaccination, in comparison to *IGHV1-69*-encoded bnAbs from HCV patients. Global B cell repertoire analysis confirmed the expansion of *VH1.36*-derived B cells in immunized animals. Most E2-specific, *VH1.36*-encoded antibodies cross-neutralized HCV. Crystal structures of two RM bnAbs with E2 revealed that the RM bnAbs engaged conserved E2 epitopes using similar molecular features as human bnAbs but with a different binding mode. Longitudinal analyses of the RM antibody repertoire responses during immunization indicated rapid lineage development of *VH1.36*-encoded bnAbs with limited somatic hypermutation. Our findings suggest functional convergence of a germline-encoded bnAb response to HCV Env with implications for vaccination in humans.

INTRODUCTION

Elicitation of broadly neutralizing antibodies (bnAbs) that can cross-neutralize diverse viral strains is a major goal for development of a hepatitis C virus (HCV) vaccine (Kinchen et al., 2018). Most bnAbs isolated from HCV-infected patients bind to a conserved antigenic surface known as the E2 neutralizing face (E2 NF), which overlaps the CD81 receptor binding site (reviewed in Tzarum et al., 2018). E2 NF is an excellent target for rational HCV vaccine design and is composed of three overlapping neutralizing sites: antigenic sites AS412, AS434, and antigenic region 3 (AR3, representing a cluster of discontinuous epitopes formed by the E2 front layer and CD81 binding loop). Virus escape studies indicate that bnAbs targeting AR3 have a high barrier to resistance (Velázquez-Moctezuma et al., 2019). AR3-specific bnAb responses have been reported in multiple individuals and are preferentially encoded by *IGHV1-69* (Bailey et al., 2017; Colbert et al., 2019; Giang et al., 2012; Keck et al., 2019; Law et al., 2008; Merat et al., 2019; Merat et al., 2016), which is a human immunoglobulin (Ig) heavy chain variable gene (IGHV or VH) frequently used against other viruses, e.g., influenza A virus and HIV-1 (reviewed in (Chen et al., 2019). These observations suggest that such antibodies can be reproducibly induced in the general population by a germline-targeting vaccine strategy. Furthermore, several studies demonstrated that *IGHV1-69*-encoded bnAbs are associated with natural clearance in HCV patients (Bailey et al., 2017; Merat et al., 2019; Merat et al., 2016) and can protect animals from HCV challenge (de Jong et al., 2014; Giang et al., 2012; Law et al., 2008). Therefore, a vaccine-induced antibody response

that effectively activates the *IGHV1-69* germline gene will likely be protective.

IGHV1-69-encoded HCV bnAbs targeting AR3 share common features for E2 NF recognition: (1) the majority of the interactions are mediated by the heavy chain; (2) an unusually hydrophobic heavy-chain complementarity-determining region 2 (CDRH2) interacts with a hydrophobic patch on E2 NF; and (3) a relatively low level of somatic hypermutation (SHM) is sufficient for antibody maturation and function (Chen et al., 2019; Flyak et al., 2018; Keck et al., 2016; Krey et al., 2013; Tzarum et al., 2020; Tzarum et al., 2019). An intramolecular disulfide within a long CDRH3 loop is found in several *IGHV1-69*-encoded bnAbs (Flyak et al., 2018; Flyak et al., 2020; Kong et al., 2013; Tzarum et al., 2019) although it is not ubiquitous (Keck et al., 2019; Law et al., 2008; Tzarum et al., 2020). Notably, E2 NF is structurally flexible (Kong et al., 2016b) and two conformations, 'A' and 'B', are recognized by different *IGHV1-69*-encoded bnAbs (Tzarum et al., 2020). Consequently, the *IGHV1-69*-encoded bnAbs can adopt different modes to recognize this flexible antigenic surface (Figure S1) (Flyak et al., 2018; Kong et al., 2013; Tzarum et al., 2020; Tzarum et al., 2019).

A comprehensive understanding of how HCV bnAbs are generated is essential for HCV vaccine design. Previous advances in next-generation sequencing (NGS) of Ig transcripts with longitudinal sampling have allowed high-resolution characterization of antibody repertoires (i.e., initial VDJ recombination, CDRH3 length, and SHM frequency) and their developmental pathways during infection and vaccination (Dai et al., 2015; Gao et al., 2019; Kong et al., 2016a; Umotoy et al., 2019; Wen et al., 2020; Wu et al., 2015). Such information is crucial for B cell lineage (or ontogeny)-based vaccine design but is not yet available for HCV bnAbs.

Rhesus macaques (RMs) provide an attractive preclinical nonhuman primate (NHP) model for evaluation of human vaccine candidates because of their genetic relatedness to humans (Ramesh et al., 2017). The VH genes of RM and human share 92% homology on average (Sundling et al., 2012a). In a previous study, we immunized four RMs with the Chiron recombinant E1E2 complex from a genotype 1a strain HCV-1 and compared the antibody responses to that of healthy volunteers immunized with the same antigen in a phase I clinical trial (Chen et al., 2020). The animals faithfully recapitulated human antibody responses to HCV Env vaccination. Although the immune sera are mostly strain-specific, bnAbs against AR3 isolated from multiple animals are mostly derived from *VH1.36*, an ortholog of the human *IGHV1-69* gene (Chen et al., 2020). To further our understanding of how HCV bnAbs are elicited by vaccination, we investigated the genetic, structural, and evolutionary bases for their elicitation in the RM model. Crystal structures of two *VH1.36*-encoded bnAbs, RM02-01 and RM11-43, with the E2 core domain indicated that they share common features for E2 NF recognition with human IG *IGHV1-69*-encoded HCV bnAbs. Lineage tracing of these RM bnAbs revealed rapid development with limited SHM. A single serine to isoleucine substitution at position 31 (S31I) in CDRH1 of the precursor antibody is sufficient for high-affinity binding and broad neutralization. These findings elucidate how *VH1.36*-encoded bnAbs were generated in HCV Env-immunized RMs by targeting the same E2 antigenic surface as human *IGHV1-69* bnAbs.. Such functional convergence of a germline-encoded bnAb response in primates has direct implications for use of the RM model in germline-targeting vaccine approaches.

RESULTS

HCV Env immunization elicited a *VH1.36*-derived B cell response in multiple RMs

To understand fundamental aspects of vaccine-elicited antibody responses in RMs, we examined circulating B cell repertoires of four animals from a previous HCV Env immunization study (Chen et al., 2020). Before immunization (week 0), the animals displayed a similar profile for VH gene usage, SHM, and CDRH3 length (Figures S2A–S2D). The VH4 family was most prevalent, followed by VH3 and VH1. In healthy human repertoires, VH3 is the predominant gene family, followed by VH4 and VH1 (Briney et al., 2019; DeWitt et al., 2016; Tzarum et al., 2019). Approximately 2%–7% of peripheral B cells in the RMs carry B cell receptors (BCR) derived from the *VH1.36* gene (Figure S2A), compared to ~4%–9% of *IGHV1-69*-derived B cells in healthy human circulating repertoires (Briney et al., 2019; DeWitt et al., 2016; Tzarum et al., 2019).

After immunization, three animals (I.D. #30734, #31881 and #31782) developed a prolonged autologous serum nAb response that peaked after the 4th immunization, whereas animal #31859 mounted a weak nAb response after the 3rd and no neutralizing activity after the 4th immunization (Chen et al., 2020). We analyzed the dynamics of global VH repertoire for #30734 and #31881 by longitudinal NGS (Figure 1A and Table S1). During immunization, VH4-derived B cells were still dominant in the RM B cell repertoires (Figures 1B, S2E, and S2F). Notable B cell expansions were observed for *VH1.36* and *VH4.40* (ortholog of human *IGHV4-39*) for #30734, and *VH5.7* (ortholog of human *IGHV5-51*) and *VH1.36* for #31881 (Figures 1B–1D). Similar to their serum nAb responses, the expansion of *VH1.36*-derived B cells peaked after the 4th immunization for both animals; at week 29, day 4 post boost, their frequency was 17% for #30734 and 5.2% for #31881. However, at week 30, their frequency rapidly decreased to 4.4% and 1.8%, respectively. Such a transient response is consistent with the dynamics of antigen-specific antibody secreting cells (ASC) elicited by the immunization (Figure 1E) (Chen et al., 2020), suggesting that the *VH1.36*-derived B cells were mostly ASC or plasmablasts. We noted a longer CDRH3 loop in the B cells from the week-29 repertoire, compared to the week-0 repertoire, for #30734, but not for #31881 (Figure 1F). No difference in overall SHM was observed for the two animals at week 0 versus week 29 (Figure 1G).

To investigate the antigen-specific B cell repertoire, we analyzed E2-sorted memory B cells of #31782 and #31859 at day 10 after the 4th immunization (Figure S3 and Table S1). At this time point, the #31782 serum nAb response reached a peak, while no neutralizing activity was detected in the #31859 serum (Chen et al., 2020). The two animals exhibited distinct B cell repertoire profiles (Figure S3). *VH1.36*- and *VH3.58*-derived B cells (contributing to 32% and 19% of total antigen-specific B cells, respectively) were dominant in the memory B cell repertoire of #31782, whereas the #31859 repertoire was largely comprised of antigen-specific B cells derived from *VH5.7*

Please cite this article in press as: Chen et al., Functional convergence of a germline-encoded neutralizing antibody response in rhesus macaques immunized with HCV envelope glycoproteins, Immunity (2021), https://doi.org/10.1016/j.immuni.2021.02.013

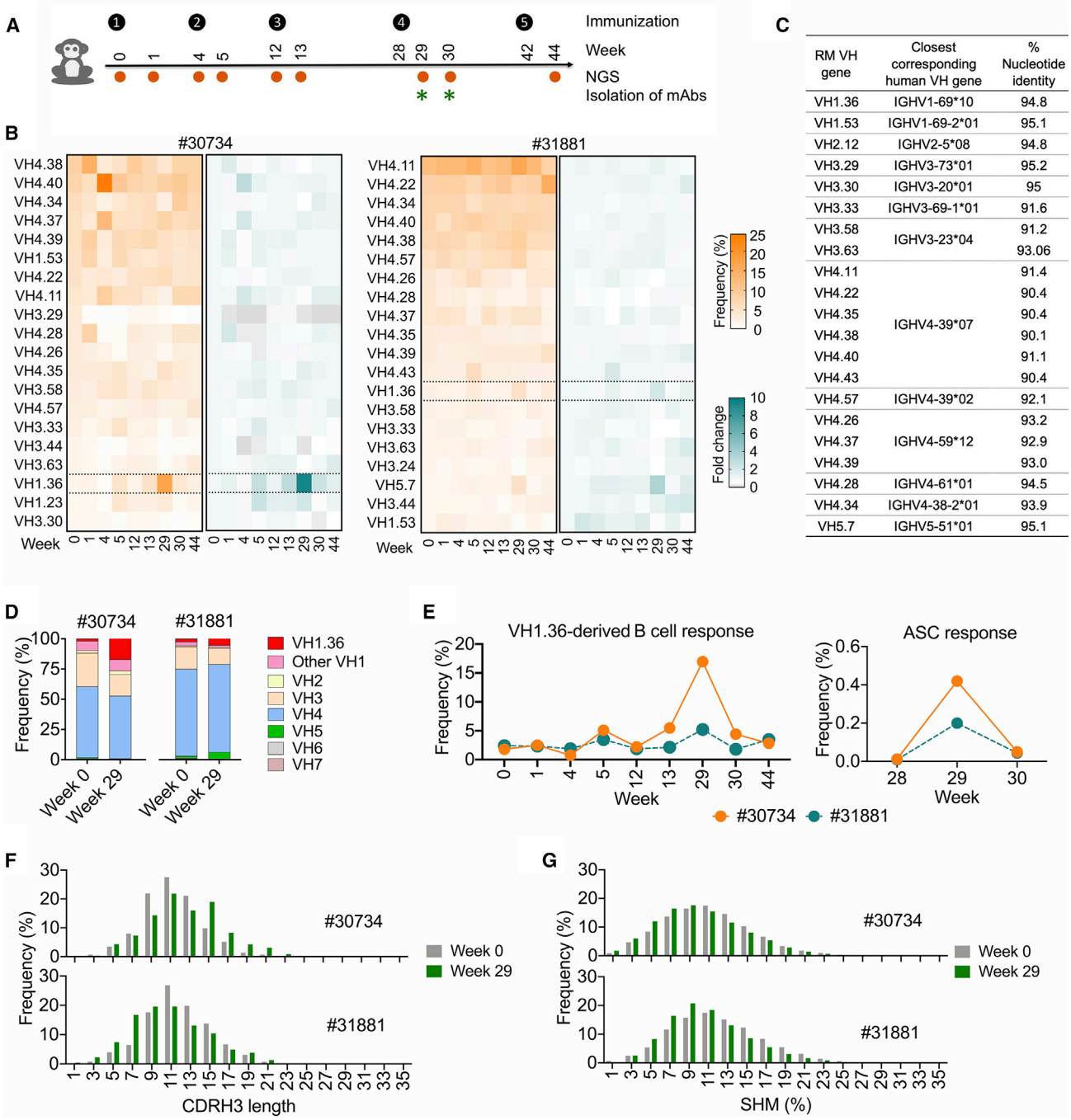

RM VH gene	Closest corresponding human VH gene	% Nucleotide identity
VH1.36	IGHV1-69*10	94.8
VH1.53	IGHV1-69-2*01	95.1
VH2.12	IGHV2-5*08	94.8
VH3.29	IGHV3-73*01	95.2
VH3.30	IGHV3-20*01	95
VH3.33	IGHV3-69-1*01	91.6
VH3.58	IGHV3-23*04	91.2
VH3.63		93.06
VH4.11	IGHV4-39*07	91.4
VH4.22		90.4
VH4.35		90.4
VH4.38		90.1
VH4.40		91.1
VH4.43		90.4
VH4.57	IGHV4-39*02	92.1
VH4.26	IGHV4-59*12	93.2
VH4.37		92.9
VH4.39		93.0
VH4.28	IGHV4-61*01	94.5
VH4.34	IGHV4-38-2*01	93.9
VH5.7	IGHV5-51*01	95.1

Figure 1. Dynamics of global B cell VH repertoires in RMs #30734 and #31881 during HCV Env immunization

(A) Schematic overview of HCV Env immunization and longitudinal sampling for RMs #30734 and #31881. The animals were immunized 5 times with recombinant E1E2, and blood samples were collected one or two weeks after each immunization. The antibody heavy chain sequences of circulating B cells were determined by next-generation sequencing (NGS), and monoclonal antibodies (mAbs) were isolated from single B cells at specified time points.

(B) Dynamics of the most frequently used VH genes in the B cell repertoires of #30734 and #31881 during the immunization. Data on *VH1.36* are highlighted by dotted lines. See also Figures S2E and S2F.

(C) The most frequently used RM VH genes and the corresponding human VH genes (Sundling et al., 2012a).

(D) Distribution of VH families at week 0 and week 29.

(E) Dynamics of *VH1.36*-derived B cell response and the E1E2-specific antibody secreting cell (ASC) response during the immunization. The data on the ASC response as previously reported (Chen et al., 2020) were included here for comparison.

(F and G) Distribution of CDRH3 length (F) and VH somatic hypermutation (SHM; G) at week 0 and week 29. CDRH3 length was based on Kabat numbering, which is 2 amino acids shorter than that in the IMGT definition. SHM is shown at the nucleotide level.

(49%) and *VH4.40* (17%). Collectively, these data demonstrated that HCV Env immunization elicited a *VH1.36*-derived B cell response related to serum neutralization in 3 of 4 RMs (#30734, #31881, and #31782).

RM *VH1.36*-encoded antibodies effect cross-neutralizing responses to HCV Env immunization

A panel (n = 100) of antigen-specific monoclonal antibodies (mAbs) were isolated from single plasmablasts and memory B cells of the week-29 and week-30 repertoires of #30734 and #31881 (Chen et al., 2020 and this study). The *VH1.36*-encoded mAbs accounted for 20% (11/56) and 7% (3/44) of total mAbs for #30734 and #31881, respectively (Figure 2A). About 71% of the *VH1.36*-encoded mAbs were capable of cross-neutralizing > 50% isolates on a panel of 14 viruses from at least five major genotypes in HCV pseudoparticles (HCVpp) and/or cell culture (HCVcc) systems, whereas 14% had limited breadth and 14% showed no neutralizing activity (Figures 2A and 2B and S4). In contrast, antigen-specific antibodies originating from the VH4 and VH3 families were mostly non-neutralizing (Figures 2A and 2B). Among the eight broadest RM bnAbs, seven originated from *VH1.36* (Figure S4A) and displayed high binding affinity (0.1-120 nM) and neutralization against diverse viruses spanning genotypes 1 to 6 (Figures 2C and 2D).

RM *VH1.36*- and human *IGHV1-69*-encoded bnAbs target overlapping epitopes and share common genetic features

We showed previously that RM *VH1.36*-encoded bnAbs competed with human AR3-specific mAb AR3A and block CD81 binding to E1E2 (Chen et al., 2020), suggesting that they target overlapping epitopes on E2 NF. Here, alanine scanning mutagenesis demonstrated that residues within HCV E2 front layer (resides 427-430 and 436-445), CD81 binding loop (residues 527 and 529), and back layer (residue 616), were critical for binding of this class of antibodies (Figure 2E).

The RM *VH1.36*- and human *IGHV1-69*-encoded bnAbs share sequence similarity particularly in CDRH2 (Figures 3A and 3B). A hallmark feature of human *IGHV1-69*-encoded bnAbs is the unusually hydrophobic tip of CDRH2 that can interact with conserved epitopes in diverse viral antigens (Chen et al., 2019; Ekiert et al., 2009; Lang et al., 2017; Lingwood et al., 2012; Tzarum et al., 2020; Tzarum et al., 2019). For most RM *VH1.36*-encoded bnAbs, a germline-encoded hydrophobic motif, $I^{51}I^{52}P^{52a}L^{53}$ (Kabat numbering), and a somatically mutated X^{54} were observed at the CDRH2 tip (Figures 3A and 3B). Both human (except for HC84.1, which binds AS434 instead of AR3) and RM antibodies had medium to long CDRH3 of 14-21 amino acids (aa; Figures 3A and 3C), compared to the 9-15 aa for naive animals (Figure S2C) and healthy human donors (Briney et al., 2019). Some human *IGHV1-69*-encoded bnAbs (e.g., AR3A, AR3C, AR3X, HEPC3, HEPC74, and HC-11) utilize the *DH2-15* or *DH2-21* segment and contain a disulfide motif (CxGGxC) that may help stabilize their CDRH3 (Figure 3A) (Flyak et al., 2018; Keck et al., 2019; Kong et al., 2013; Tzarum et al., 2019). However, such a motif was not observed in AR3B, AR3D, HC-1AM, 212.1.1, 212.10 and HC84.1, or in the RM bnAbs here (Figure 3A). The SHM in the VH of RM *VH1.36*-encoded bnAbs ranged from 4%–8% (average 6%) at the nucleotide level (Figures 3A and 3C), whereas human *IGHV1-69*-encoded bnAbs appeared to have a higher SHM (Figure 3C), likely due to continuous stimulation by evolving virus during chronic infection. In summary, the genetic features of RM *VH1.36*-encoded bnAbs were similar to human *IGHV1-69*-encoded bnAbs.

Crystal structures of RM *VH1.36*-encoded bnAbs in complex with E2

To further characterize E2 recognition by RM *VH1.36*-encoded bnAbs, we determined the crystal structure of the Fab fragments of antibodies RM2-01 and RM11-43 (both isolated from #30734) in complex with the E2 core domain (recombinant E2c3 protein) of HCV isolate HK6a (Bukh et al., 2010; Meunier et al., 2005; Tzarum et al., 2019) (Table S2). The structures elucidated that RM2-01 and RM11-43 bound to epitopes that overlap with AR3 (Figure 4A), consistent with the epitope mapping data (Figure 2E). The two antibodies represented two distinct B cell lineages in the panel of RM *VH1.36*-derived bnAbs (Figure 3A) (Chen et al., 2020). Sequence alignment of the RM2-01 and RM11-43 VH regions (aa 1-113) showed high sequence identity in their CDRH1 and CDRH2 loops (100% and 88%, respectively), but notable difference in their CDRH3 sequence and length (15 versus 19 aa, Figure S5A). Superposition of the two complexes revealed that RM2-01 and RM11-43 bind E2 in a similar overall orientation (Figure S5B). However, major conformational differences in CDRH3 as well as minor variations in CDRH2 were observed between the two complexes (Figures S5B and S5C), whereas HK6a E2c3 remained largely unchanged (Figure S5D) with a Cα RMSD of 0.38Å on 127 residues. Buried surface area (BSA) analysis indicated that the majority of the E2 epitope surface area was buried by the VH region (620 $Å^2$ by RM2-01 and 790 $Å^2$ by RM11-43 VH, equivalent to 87% of the total BSA [712 and 907 $Å^2$, respectively] for both antibodies; Figures 4B and S5E). Consistently, as indicated by biolayer interferometry (BLI), the swapping of the wild-type light chains with other unrelated light chains did not compromise their binding affinity for E2 (Figure 4C).

Detailed analysis of the interactions between RM2-01 and RM11-43 antibodies to HK6a E2c3 revealed that, for both antibodies, the CDRH1 loops formed hydrophilic charged (salt bridge and/or π-cation) and hydrophobic interactions with the front layer and CD81 binding loop, whereas the CDRH2 loops only engage in side-chain hydrophobic interactions with the front layer (Figures 4D and 4E). Both CDRH3s formed hydrophobic interactions and main-chain hydrogen bonds with the front and back layers. Due to low sequence similarity and differences in CDRH3 loop length (15 versus 19 aa) and conformation (Figures S5A and S5C), the CDRH3 of each mAb created a different set of interactions (Figures 4D, 4E, and S5F). Interestingly, the CDRH3 loops of both RM2-01 and RM11-43 made direct contacts with the back layer (Y613 and P612, respectively).

Structural comparison of E2 recognition by RM *VH1.36*- versus human *IGHV1-69*-encoded bnAbs

E2 recognition by human *IGHV1-69*-encoded bnAbs has been well described (Flyak et al., 2018; Flyak et al., 2020; Kong et al., 2013; Tzarum et al., 2020; Tzarum et al., 2019), revealing common binding features as well as different binding modes based on relative CDR dispositions, angles of approach, and interacting E2 residues (Figure S1). Structure elucidation of HK6a

Please cite this article in press as: Chen et al., Functional convergence of a germline-encoded neutralizing antibody response in rhesus macaques immunized with HCV envelope glycoproteins, Immunity (2021), https://doi.org/10.1016/j.immuni.2021.02.013

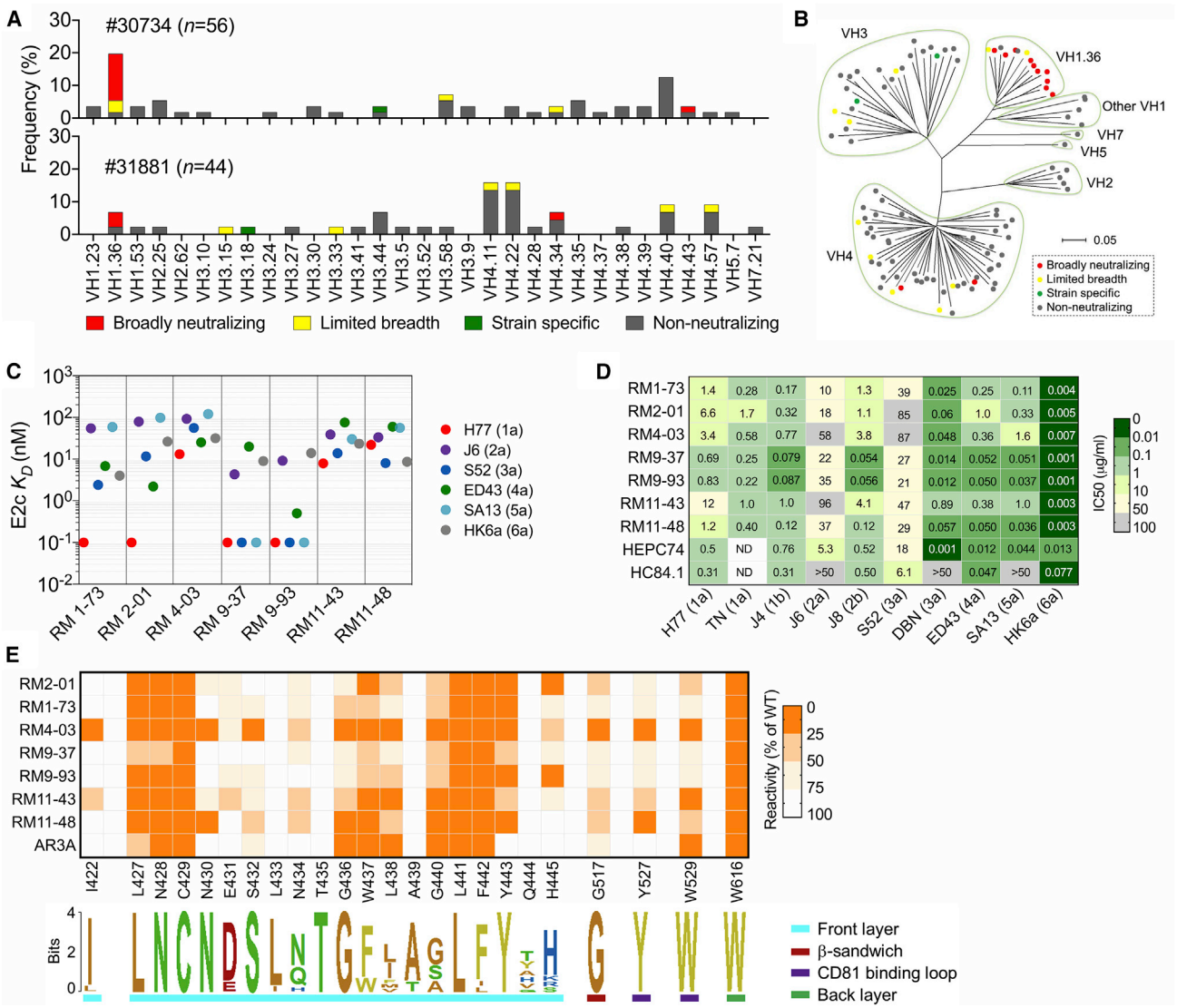

Figure 2. Function and specificity of RM *VH1.36*-encoded bnAbs

(A) VH gene usage of antigen-specific mAbs isolated from RMs #30734 and #31881. Neutralization breadth is defined as the percentage and genotype of viruses neutralized by the mAbs using a panel of 7 HCVpp and 12 HCVcc. Neutralizes > 50% of viruses from at least five genotypes, broadly neutralizing; neutralizes 8%–50% viruses, limited breadth; neutralizes only 1 virus, strain-specific. See also Figure S4A.

(B) Maximum likelihood (ML) tree of heavy chain aa sequences of the RM mAbs.

(C) Binding affinity of *VH1.36*-encoded bnAbs to HCV E2 core (E2c) from genotypes 1-6 by biolayer interferometry (BLI).

(D) Neutralization breadth and potency of *VH1.36*-encoded bnAbs against 10 HCVcc. Human *IGHV1-69*-encoded bnAbs HEPC74 and HC84.1 were included as controls. Half-maximum inhibitory concentration (IC_{50}) is shown in μg/mL. ND, not determined.

(E) Epitope mapping of *VH1.36*-encoded bnAbs by alanine scanning mutagenesis. Cells show binding percentage relative to wild type H77. The E2 sequence logo of the 14 viruses (HCV-1, H77, TN, DH1, UKN1B.12.6, J4, J6, J8, S52, DBN, ED43, UKN4.11.1, SA13, and HK6a) used in this study are shown.

See also Figure S4B.

E2c3-RM2-01 and HK6a E2c3-RM11-43 complexes enabled detailed comparison of E2 recognition by RM *VH1.36*- and human *IGHV1-69*-encoded bnAbs. Despite variation in their germline sequences, the human and RM bnAbs share a similar hydrophobic CDRH2 tip for antigen interaction that is dominated by the heavy chain (Figure 3A). Structural comparison of RM2-01 and RM11-43 with representative human *IGHV1-69*-encoded bnAbs (AR3A for AR3A/B/C/D, U1 and HC-11 group; 212.1.1 for 212.1.1 and HC-1AM group; HEPC74 for HEPC74 and HEPC3 group) (Flyak et al., 2018; Tzarum et al., 2020; Tzarum et al., 2019) illustrated that these two RM bnAbs bound to an antigenic surface overlapping with the epitopes recognized by the human bnAbs (Figures 5A and 5B). However, variation in the angle of Fab approach to E2 resulted in notable differences in the CDRH footprint (Figure S6). The CDRH3 loops of human *IGHV1-69*-encoded bnAbs interact with an exposed surface formed by the front layer and CD81 binding loop, whereas their CDRH2 (except for HEPC3/74) engage with a hydrophobic

Please cite this article in press as: Chen et al., Functional convergence of a germline-encoded neutralizing antibody response in rhesus macaques immunized with HCV envelope glycoproteins, Immunity (2021), https://doi.org/10.1016/j.immuni.2021.02.013

A

	mAb	Donor	D gene	J gene	CDRH1 (31-35)	CDRH2 (50-65)	CDRH3 (95-102)	CDRH3 Length	% SHM	Reference
	VH1.36				SYAIS	VIIPLVGITNYAEKFQG				
RM *VH1.36*-encoded bnAbs	RM1-73	#30734	DH6-3*01	JH6*01	IS..G	E.....Q....	GDSKLQSVAAGGTEGGNGL-DS	21	4	Chen et al., 2020 and this study
	RM2-01		DH1-8*01	JH4*01	I....	E.V..G.....QN...	VRTALVGPREGIF-------DF	15	7	
	RM9-37		DH4-2*01	JH6*01	I.G..	E....A...S..Q...D	GGKKVGTLLGNYAL------DF	16	5	
	RM9-93		DH1-8*01	JH4*01	I..L.	E.V..G.L.Y..Q...D	GRTTLVGPREGIF-------DF	15	8	
	RM10-30		DH2-1*01	JH5-1*01	ID...	E...R....V..Q..HD	GQAEGSLRLRWF--------DV	14	5	
	RM11-43		DH3-1*01	JH6*01	I....	E....G.....Q....	GETKMITVLAGTTGGGL---DS	19	4	
	RM11-48		DH6-3*01	JH5-1*01	V...T	E.....Q....	GVTRIAAAGTGNWF------DV	16	5	
	RM11-60		DH4-2*01	JH6*01	I.G..	E...V..M.H..Q....	GGKKVGTLLGNYGL------DS	16	7	
	RM4-03	#31881	DH4-2*01	JH4*01	I....	G....L.TA...Q....	EGKESGYSFKNLPYF-----EY	17	7	
	RM4-07		DH2-5*01	JH5-1*01	I.G..	E....GS.....Q....	VETLIVGRGSGWF-------DV	15	7	
	IGHV1-69*01				SYAIS	GIIPIFGTANYAQKFQG				
Human *IGHV1-69*-encoded bnAbs	AR3A	Same donor	DH2-15*01	JH4*02	..S.N	TF..M...SK.....	PETPRYCSGGFCYGEF----DN	18	15	Giang et al., 2012; Law et al., 2008; Tzarum et al., 2019
	AR3B		DH3-10*01	JH5*02	E-PVT	....A..VTK.....	VGLRGIVMVGGLAMNWL---DP	19	14	
	AR3C		DH2-21*01	JH4*02	N..LN	.VV.L...TRN.....	SVTPRYCGGGFCYGEF----DY	18	14	
	AR3D		DH3-16*02	JH5*02	..V.T	A...F...T.L.....	AGDLSVGGVLAGGVPHLRHFDP	22	9	
	HEPC3	117	DH2-15*01	JH5*02	..E.T	..T...E..T.....	DGVRYCGGGRCYNWF-----DP	17	5	Bailey et al.,2017,
	HEPC74	110	DH2-15*01	JH5*02	N....	.MS..SN.PK.....	DLLKYCGGGNCHSLLV----DP	18	8	Flyak et al., 2018
	HC-1AM	Same donor	DH2-21*01	JH3*01	GEV..	VF..M..I.D.....H.	VLQVGRNLVVRPL-------DL	15	11	Tzarum et al., 2020
	HC-11		DH2-15*01	JH4*03	.FIF.	....M....K..PRL..	EVPGFCRGGSCSGYM-----DV	17	8	Keck et al., 2008
	212.1.1	Same donor	DH5-24*01	JH3*02	..G..	.S...L..SV.....	VREGMAAISGKNAF------DI	16	7	Keck et al., 2019;
	212.10		DH5-24*01	JH4*02	I.T.N	S...AV.LTD.T.....	DRMRDDSTLFRDSHF-----DN	17	11	Tzarum et al., 2020
	HC84.1	-	DH2-15*01	JH4*03	N.V.T	.F..T.R..M...G...	GPLSRGYY----------DY	10	26	Krey et al., 2013

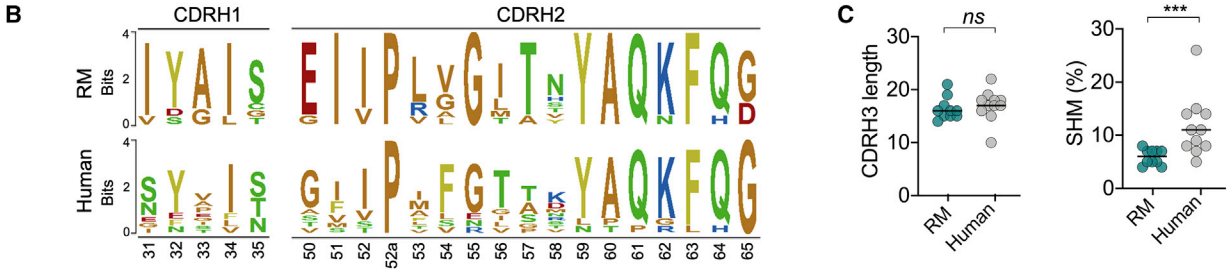

Figure 3. Comparison of genetic features of RM *VH1.36*- and human *IGHV1-69*-encoded bnAbs

(A) Heavy-chain CDR amino acid sequences, CDRH3 length, and SHM rate of individual antibodies. The germline genes *VH1.36* and *IGHV1-69*01* are shown as reference. Note that AR3C, AR3A, HC-1AM, and 212.10 are encoded by *IGHV1-69*06*, **15*, **17*, and **04*, respectively. Sequence differences between these gene alleles have been reported in (Chen et al., 2019). Dots denote matches to the reference sequence. The hydrophobic motif at CDRH2 tip and the disulfide motif (CxGGxC) in CDRH3 are in red and blue, respectively. Kabat numbering is indicated.

(B) Amino acid sequence logo of CDRH1 and CDRH2.

(C) Comparison of CDRH3 length and SHM level of RM and human antibodies. *P values* were calculated using two-tailed Mann-Whitney test. ns, not significant. ***$p < 0.0001$.

groove formed by the front layer N terminus (aa 421-428), helix α1 C terminus (aa 442-443), and CD81 binding loop tip (W529) (Figure 5B). In contrast, CDRH3 of RM2-01 and RM11-43 interacted with the hydrophobic groove, whereas CDRH2 only contacted hydrophobic residues of helix α1 (aa 438-443).

CDRH3 of RM2-01 and RM11-43 also interacted with the α2 helix of the back layer (aa 614-617; Y613 for RM2-01 and P612 for RM11-43) (Figures 4D and 4E) that contains residues critical for CD81 receptor binding (Y613 and W616) (Gopal et al., 2017; Roccasecca et al., 2003). In most E2-bnAb structures, the α2 helix region is shielded by the front layer and only partially exposed, and therefore unable to interact with bnAbs. In our structures of H77 E2c3-Fab 212.1.1 and H77 E2c3-Fab HC-1AM, the E2 front layer adopts a different conformation that exposes the helix α2 region (termed 'B' conformation), allowing interaction of the antibodies with two back layer residues, Y613 and W616 (Figure 5A) (Tzarum et al., 2020). Superposition of E2 from HK6a E2c3-RM2-01 and HK6a E2c3-RM11-43 on H77 E2c3-AR3A ('A' conformation) and H77 E2c3-212.1.1 ('B' conformation) indicated that the two RM bnAbs bound to the E2 'A' conformation (Figure 5C), suggesting that the interactions with the back layer α2 helix were a result of the unique angle of approach for RM2-01 and RM11-43.

Analysis of the human bnAb structures indicated that the CDRH2 tips of the AR3A-like bnAbs were positioned vertical to the hydrophobic groove and interacted with both front layer and CD81 binding loop (Figure 5D). For 212.1.1 and HC-1AM, as a result of changes in the front layer conformation, CDRH2 bound more deeply into the hydrophobic groove and engaged the front layer, CD81 binding loop, and back layer α2 helix (Figure 5D). In contrast, CDRH2 of RM2-01and RM11-43 was positioned parallel to the surface of the front layer and used residues upstream to the tip to interact only with the front layer, similar to interactions observed for HEPC3/74 CDRH2 (Figure 5D).

RM *VH1.36*-encoded bnAbs require only a few SHMs for partial or full function

The heavy chains of RM2-01 and RM11-43 differed from their inferred germline precursors (GLs) by 14 (11.3%) and 7 (5.5%) aa,

Please cite this article in press as: Chen et al., Functional convergence of a germline-encoded neutralizing antibody response in rhesus macaques immunized with HCV envelope glycoproteins, Immunity (2021), https://doi.org/10.1016/j.immuni.2021.02.013

CellPress

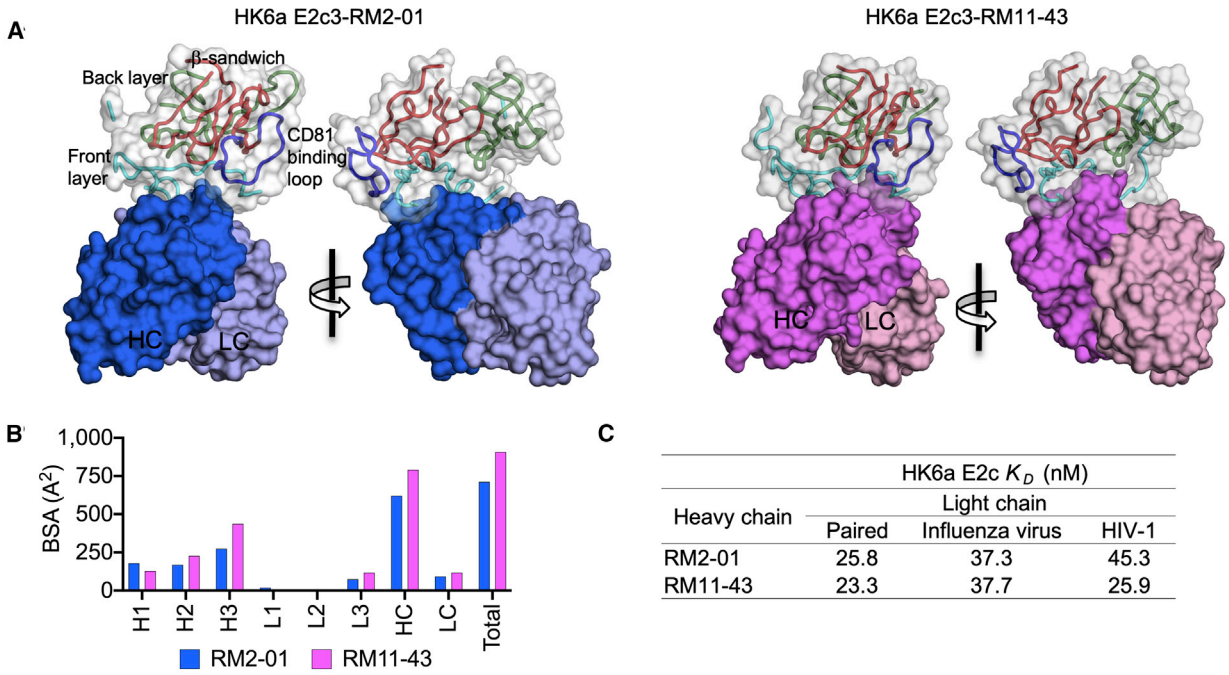

C

Heavy chain	HK6a E2c K_D (nM)		
	Light chain		
	Paired	Influenza virus	HIV-1
RM2-01	25.8	37.3	45.3
RM11-43	23.3	37.7	25.9

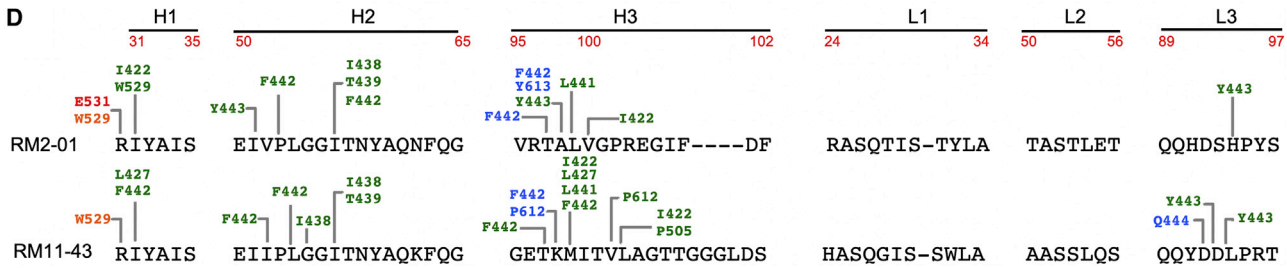

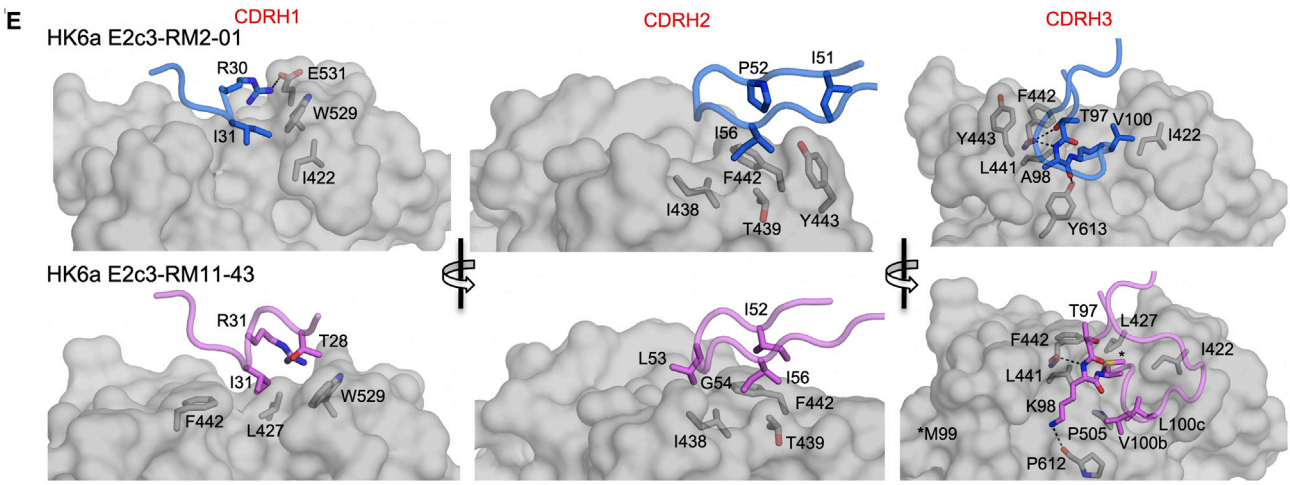

Figure 4. Crystal structures of HK6a E2c3-RM *VH1.36*-encoded nAb complexes

(A) Crystal structures of HK6a E2c3-RM2-01 (blue) and HK6a E2c3-RM11-43 (pink) complexes. For clarity, only the Fab variable regions are shown.

(B) Buried surface area (BSA) by the CDRs of RM2-01 and RM11-43 mAbs on HK6a E2c3. See also Figure S5E. (C) Biolayer interferometry (BLI) binding affinity of RM2-01 and RM11-43 to HK6a E2c, where their light chains were swapped with light chains from an anti-influenza virus antibody or HIV-1 antibody.

(legend continued on next page)

Please cite this article in press as: Chen et al., Functional convergence of a germline-encoded neutralizing antibody response in rhesus macaques immunized with HCV envelope glycoproteins, Immunity (2021), https://doi.org/10.1016/j.immuni.2021.02.013

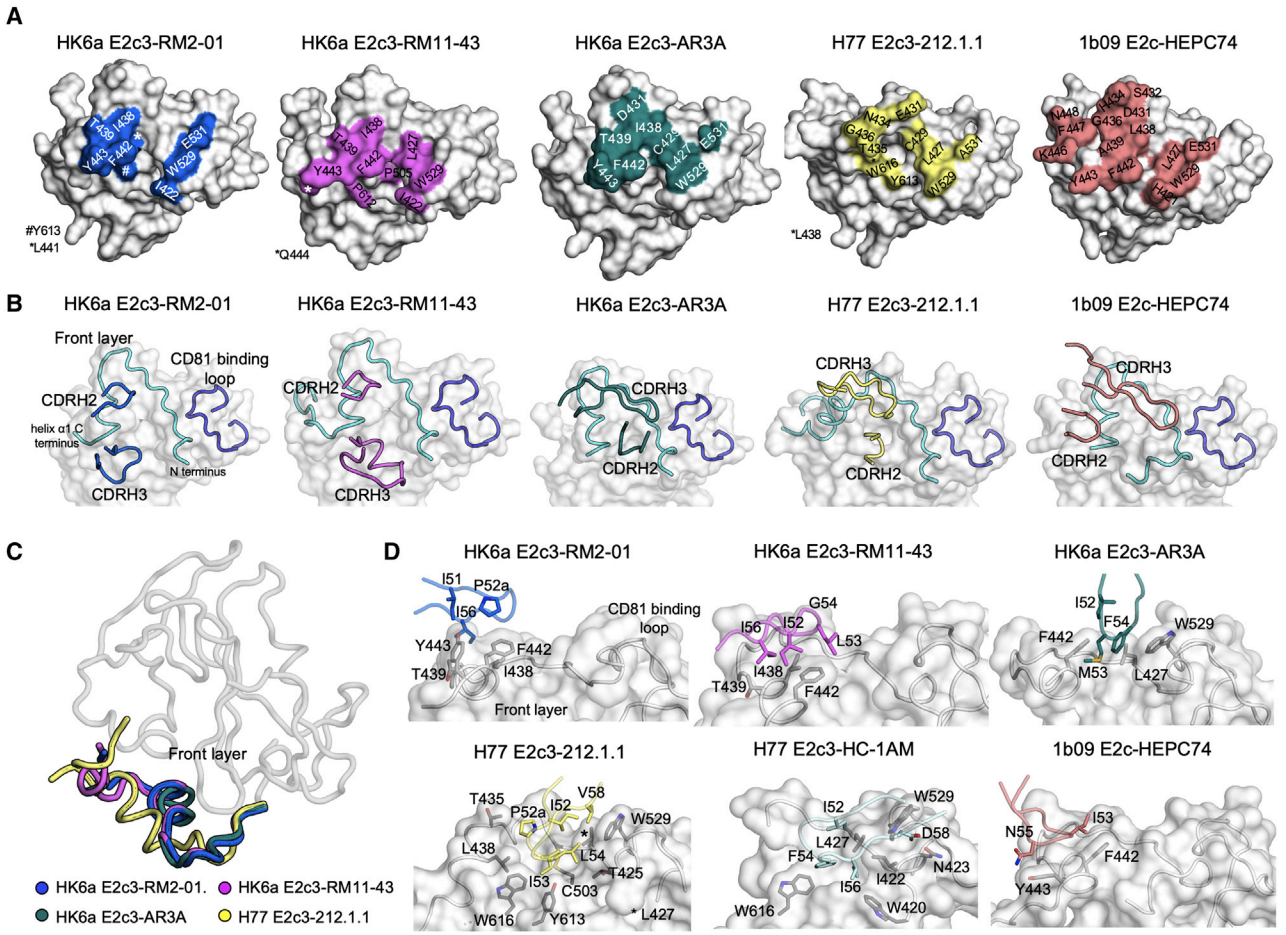

Figure 5. Comparison of E2 complex structures with RM *VH1.36*-encoded versus human *IGHV1-69*-encoded bnAbs

(A) Comparison of RM2-01 (blue), RM11-43 (violet), AR3A (teal), 212.1 (yellow), and HEPC74 (salmon) epitopes. The E2c structures are shown in surface representation and the interacting residues are colored and labeled.

(B) The position of the CDRH2 and CDRH3 in the E2c3-Fab structures. The E2c3 is shown in surface presentation with the front layer and CD81 binding loop as a cartoon and colored by cyan and blue, respectively. The CDRH2 tip (aa 51-56) and CDRH3 are shown in cartoon representation.

(C) Superposition of E2 from RM2-01, RM11-43, AR3A, and 212.1.1 complexes indicating similarity of the front layer conformation in RM2-01 and RM11-43 complexes to that of the AR3A complex.

(D) Interactions between E2 (gray) and CDRH2 of *VH1.36*-encoded or representative *IGHV1-69*-encoded bNAbs. Interacting residues are labeled and shown in stick representation.

respectively (Figure 6A). Mutations were observed in framework (FR) 1, CDRH1, CDRH2, FR3, and CDRH3. Only a few (2 for RM2-01 and 4 for RM11-43) appeared to have direct interactions with E2 NF: R30 (FR1) and I31 (CDRH1) were shared by both antibodies, and G54 (CDRH2) and K98 (CDRH3) were in RM11-43 only (Figures 4D and 4E). To examine the minimum requirements for affinity maturation, we compared the inferred heavy chain GLs for RM2-01 and RM11-43, as well as a GL with mature CDRH3 (GM), to the affinity-matured antibodies (MA) (Figure 6A). We also created heavy-chain GM and MA variants by substituting somatic mutations singly or in combination, with a focus on the epitope-contacting CDRs and residues at the hydrophobic CDRH2 tip. The heavy chain variants were paired with their corresponding mature light chains and tested for their ability to bind and neutralize diverse HCV isolates.

For both antibodies, GL, GM and GM(G30R) variants showed little activity toward the isolates tested (Figures 6B–6E). Instead, high binding affinity for both autologous and heterologous viruses was achieved with an S31I substitution in CDRH1 (Figures 6B–6E). S31I, together with R30G and R30G/G54V/K98R for RM2-01 and RM11-43, respectively, enabled broad binding against heterologous viruses. Consistently, reversion of the

(D) Schematic overview of the interactions between HK6a E2c and RM2-01 and RM11-43 heavy chains. The CDR sequences were aligned, and E2 interacting residues are highlighted here in red (salt bridge) orange (pi-cation) blue (hydrogen bonds) and green (hydrophobic interactions).

(E) Interactions between E2 (gray) and CDRH1-3 of RM2-01 (blue) and RM11-43 (pink). The interacting residues are labeled and shown in stick representation and hydrogen bonds are shown as dashed lines.

Please cite this article in press as: Chen et al., Functional convergence of a germline-encoded neutralizing antibody response in rhesus macaques immunized with HCV envelope glycoproteins, Immunity (2021), https://doi.org/10.1016/j.immuni.2021.02.013

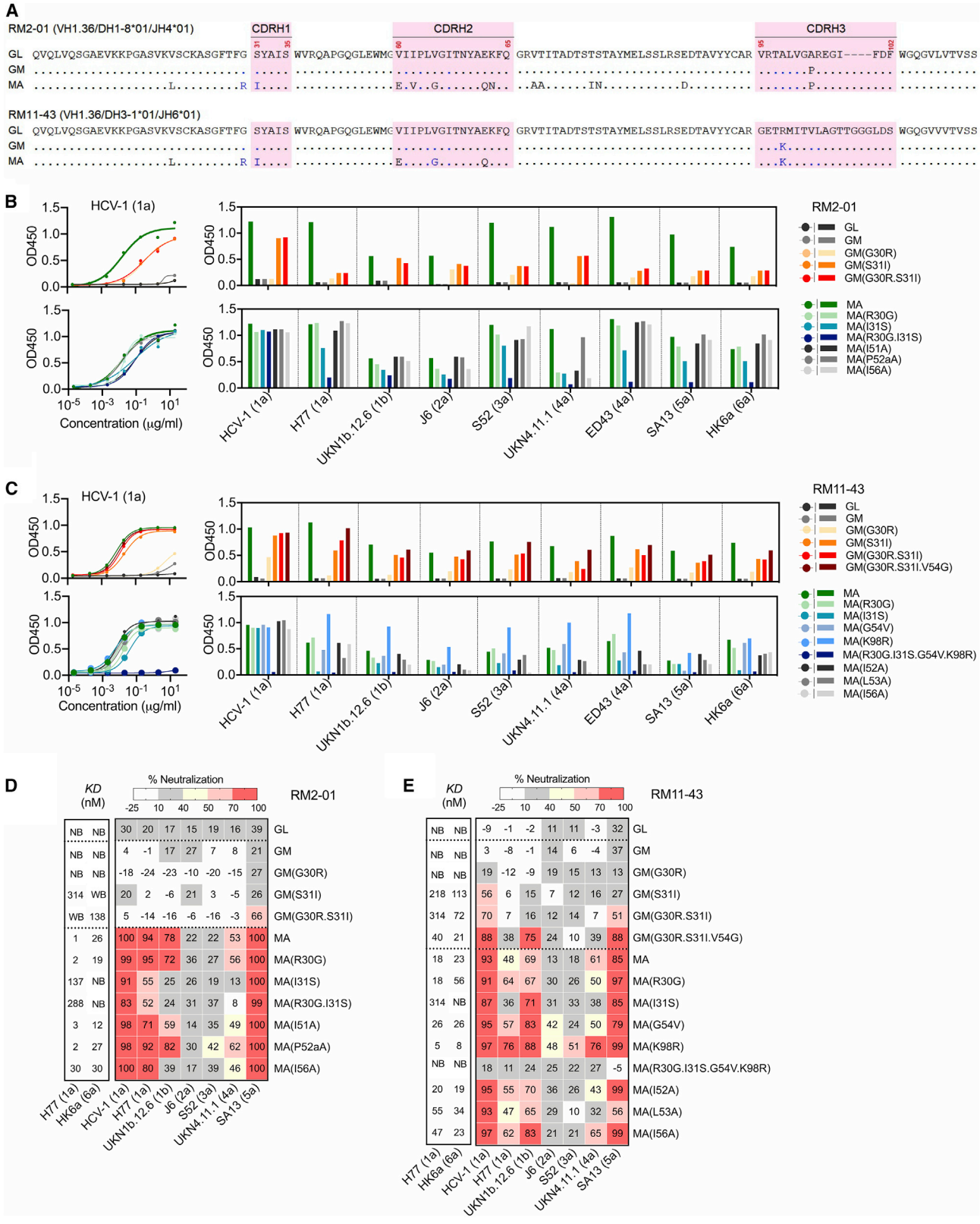

Figure 6. Effects of SHM on RM *VH1.36*-encoded bnAb function

(A) Alignment of heavy-chain aa sequences of RM2-01 and RM11-43 inferred germline precursors (GL), GL with the mature antibody CDRH3 (GM), and mature antibodies (MA). Dots denote matches to the reference sequence. Kabat numbering is indicated.

(legend continued on next page)

S31I or G30R/S31I mutations in the mature antibodies markedly decreased their binding breadth to heterologous viruses. For RM11-43, MA(G54V) slightly increased neutralization of J6, and MA(K98R) largely improved both binding and neutralization against heterologous viruses, whereas MA (R30G/I31S/G54V/K98R) greatly impaired binding and neutralization for all viruses tested. Substitution of individual residues at the CDRH2 tip with alanine (I51A and P52aA for RM2-01, I52A and L53A for RM11-43, and I56A for both antibodies) had a relatively minor effect on antibody function. Together, these results demonstrate that affinity maturation of *VH1.36*-encoded bnAbs required only a few somatic mutations in VH with a single S31I substitution in CDRH1 to confer high-affinity binding to autologous virus. As this mutation was widely present in RM *VH1.36*-encoded bnAbs (Figure 3A), it may represent a common mechanism of affinity maturation for this antibody class.

RM *VH1.36*-encoded bnAbs achieve breadth through rapid lineage development

Following identification of key residues for antigen recognition by the RM *VH1.36*-encoded bnAbs, we traced their developmental pathways to gain further insight into their ontogeny. The heavy-chain repertoires of #30734 and #31881 at 9 time points (Figure 1A) were interrogated using 10 single-cell sorted *VH1.36*-encoded bnAbs as references. Two-dimensional identity-divergence analysis and CDRH3-based lineage tracing revealed similar patterns of heavy-chain expansion for all 10 bnAbs (Figures 7A and S7). In all cases, the first notable expansion was observed after the 3rd immunization (week 13). After the 4th immunization, the response peaked at week 29, followed by a quick contraction at week 30, which was consistent with the circulating *VH1.36*-derived B cell expansion. Analysis of the repertoire NGS data from the pre-immunization and early time points (weeks 0–12) revealed highly similar heavy chains (> 90% nucleotide sequence identity) in the naive repertoire for 6 of the 10 *VH1.36*-encoded bnAbs (Figure S7) and rapid accumulation of SHMs in CDRH1 and CDRH2 for all analyzed antibodies (Figure 7B).

We then traced antibody lineages for RM2-01, RM9-93, RM11-43 and RM9-37 (the most broad and potent *VH1.36*-encoded bnAbs) in #30734. We found that RM2-01 and RM9-93 were members of the same clonal lineage based on their V and J gene usage, CDR3 length, and CDR3 sequence identity (Chen et al., 2020). B cell precursors of the RM2-01, RM9-93 and RM9-37 lineages were observed in the week 0 repertoire, whereas the RM11-43 lineage was first detected at week 1 (Figure 7A). These sequences also exhibited SHMs at key contact residues for RM2-01 and RM11-43, e.g., aa 30 in FR1, aa 31 in CDRH1, aa 54-56 in CDRH2 tip, and aa 97-100 in CDRH3 (Figure 7C).

To validate our findings from the repertoire analysis, selected heavy chains of the RM2-01, RM11-43, and RM9-37 sub-lineages from week 0 and early time points were paired with their respective light chains for functional evaluation. The reconstituted antibody variants exhibited high binding affinity and neutralization for E1E2 derived from multiple HCV isolates similar to the corresponding *VH1.36*-encoded bnAbs (Figures 7D and 7E). These data indicated that the naive RM repertoire contained BCRs that encoded high-affinity, HCV-reactive, *VH1.36* antibodies, from which a rapid response could be mounted following HCV Env immunization. These activated B cells continued to evolve and finally converged to the affinity-matured bnAbs after multiple vaccine boosts.

DISCUSSION

"Germline-endowed" antibody responses are observed not only for HCV but also for other viral pathogens, e.g., influenza virus (Joyce et al., 2016; Pappas et al., 2014; Wheatley et al., 2015), HIV-1 (Wu et al., 2011; Zhou et al., 2015), rotavirus (Di Niro et al., 2010; Weitkamp et al., 2005), and SARS-CoV-2 (Robbiani et al., 2020; Yuan et al., 2020). Because these antibodies are preferentially encoded by specific genes, it may be feasible to activate these germline pathways reproducibly to generate the desired antibody response. As these VH genes are unique to humans and are not expressed in standard animal models like rodents, designed immunogens have been only investigated in transgenic mice, e.g., for elicitation of *VH1-2*-encoded VRC01 class bnAbs against HIV-1 (Huang et al., 2020; Tian et al., 2016) and *IGHV1-69*-encoded bnAbs against influenza virus (Sangesland et al., 2019).

Human antibody responses against AR3 within HCV E2 NF are characterized by their exceptional neutralization breadth, conserved epitope targeting, low SHM, and restricted *IGHV1-69* gene usage (Chen et al., 2019). This genetic bias underscores an interesting relationship between HCV and the bnAb response that is highly relevant for rational design of a germline-targeting HCV vaccine. Some germline-reverted precursors of human *IGHV1-69*-encoded bnAbs bind HCV E2 with high affinity and neutralization breadth is acquired by affinity maturation (Flyak et al., 2018; Tzarum et al., 2019). These attributes, along with limited SHM, suggest the potential to target *IGHV1-69*-derived precursor B cells for efficient elicitation of bnAbs by vaccination. In our previous study (Chen et al., 2020), AR3-specific antibody responses can be readily elicited by HCV Env immunization in both humans and RMs, albeit at low titer. Intriguingly, the RM AR3-targeting bnAbs exhibit biased usage of *VH1.36,* which is 94.8% identical to human *IGHV1-69*. Of note, the IgBlast database (Ye et al., 2013) was used here for RM Ig gene identification and genetic assignment. The incomplete reference sequences of RM Ig alleles may affect identification of authentic SHM but will not change B cell lineage assignment as they are defined by CDRH3 sequence identity. With advances in NGS of the BCR loci of RMs, additional genes and alleles have been identified and several alleles may be associated with the *VH1.36* gene (Cirelli et al., 2019; Ramesh et al., 2017; Vigdorovich et al., 2016).

(B and C) ELISA binding of RM2-01 (B) and RM11-43 (C) antibody variants to the autologous HCV-1 (left, serial dilutions starting from 20 μg/mL) and diverse heterologous strains (right, at 20 μg/mL).

(D and E) BLI binding affinity (left) and HCVpp neutralization (right) of RM2-01 antibody variants (D) and RM11-43 antibody variants (E) against diverse HCV viral strains. Antibodies were tested at a single concentration of 50 μg/mL in HCVpp. Data shown are the average of at least 3 experiments. NB, no binding. WB, weak binding.

Please cite this article in press as: Chen et al., Functional convergence of a germline-encoded neutralizing antibody response in rhesus macaques immunized with HCV envelope glycoproteins, Immunity (2021), https://doi.org/10.1016/j.immuni.2021.02.013

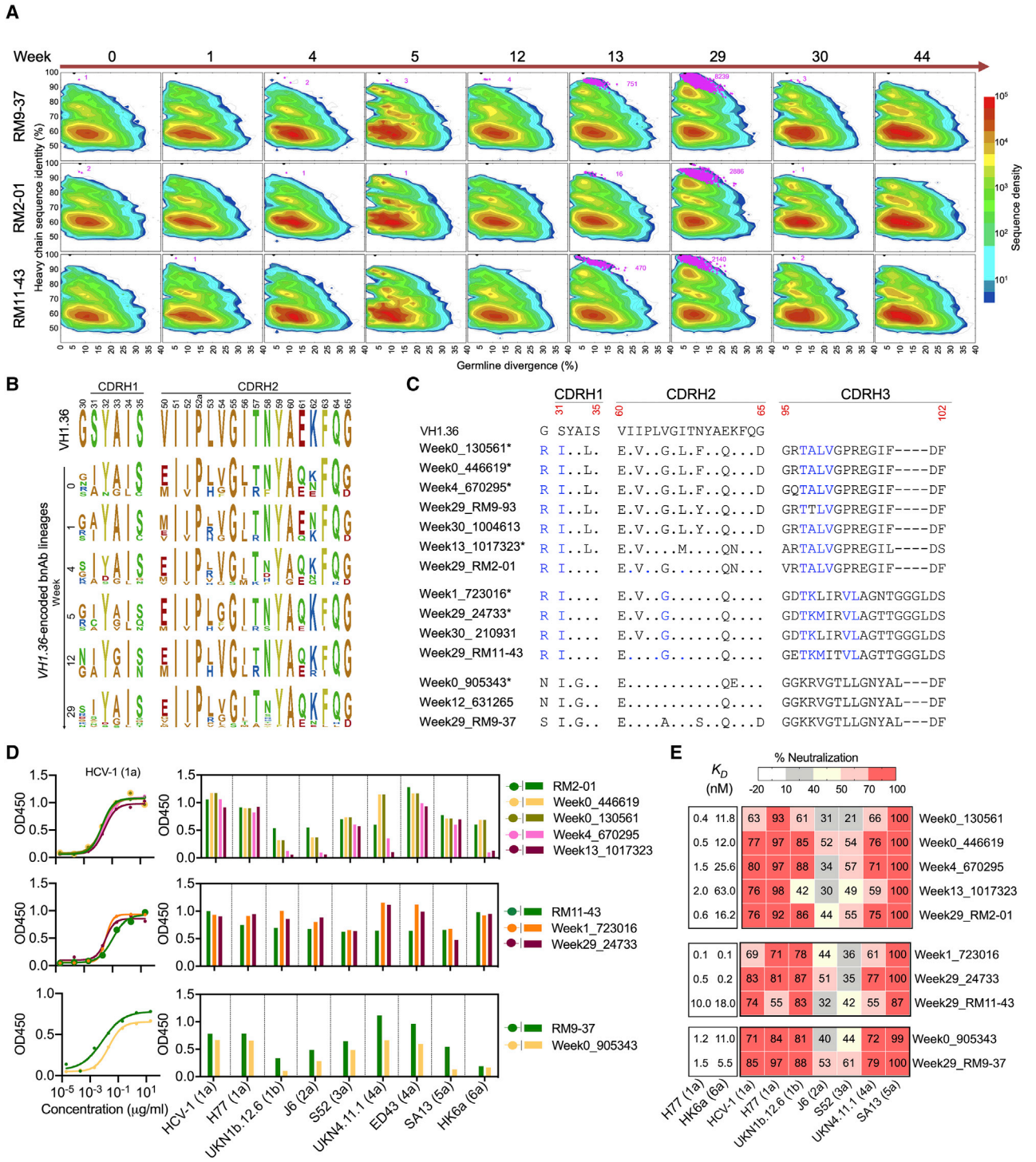

Figure 7. Longitudinal sequence analysis of the RM *VH1.36*-encoded bnAb lineages

(A) Identity-divergence analysis of the heavy chains of RM9-37-, RM2-01- and RM11-43-like antibodies in circulating B cell repertoires. Color coding denotes sequence density. See also Figure S7.

(B) CDRH1 and CDRH2 aa sequence logo of the *VH1.36*-encoded bnAb-like heavy chains identified from the NGS-derived RM B cell repertoires at early time points during the immunization.

(C) CDR sequence alignment of the RM2-01-, RM11-48-, and RM9-37-like heavy chains identified from indicated time points. Dots denote matches to the reference sequence. Epitope-interacting residues in the crystal structures are colored in blue for the RM2-01 and RM11-43 somatic variants.

(D and E) ELISA binding (D), BLI binding and HCVpp neutralization (E) of synthesized antibodies containing NGS-derived heavy chains, and RM2-01, RM11-43, or RM9-37 light chains.

Due to the lack of availability of B cells from the human subjects, we were not able to directly compare the human and RM antibody responses during the immunization. Nonetheless, comparison of bnAbs from immunized RMs with AR3-targeting bnAbs isolated from HCV-infected patients revealed functional convergence of a germline-encoded bnAb response to HCV Env in humans and RMs. The RM and human antibodies shared common features such as broad neutralizing activity, heavy-chain-mediated binding, hydrophobic motif in CDRH2, and rapid affinity maturation with limited SHM.

To counteract structural flexibility and variation in E2 NF in different HCV viruses, human *IGHV1-69*-encoded bnAbs employ different modes of recognition (Figure S1). The crystal structure of an E2 core with a *IGHV1-69*-encoded bnAb, AR3C, marked an important step toward atomic-level understanding of HCV neutralization by human bnAbs and established a critical role for the hydrophobic CDRH2 tip and a long CDRH3 in recognition of E2 NF (Kong et al., 2013). Previous structures of E2 with ten different *IGHV1-69*-encoded bnAbs that target AR3 (Flyak et al., 2018; Flyak et al., 2020; Tzarum et al., 2020; Tzarum et al., 2019) extended our understanding of HCV recognition by this class of bnAbs. These structures suggested that *IGHV1-69*-encoded bnAbs can be clustered into sub-groups based on their genetic and structural characteristics. For instance, the CDRH3s of AR3A, AR3C, HC-11, HEPC3, and HEPC74 acquire a β-hairpin conformation and contain a germline-encoded disulfide that stabilizes CDRH3. For AR3B and AR3D, CDRH3 adopts a similar conformation yet lacks the disulfide. Another feature to differentiate *IGHV1-69*-encoded bnAbs is the angle of approach and CDR footprint on E2 NF (Figure 5). Our previous study (Tzarum et al., 2020) indicates that *IGHV1-69*-encoded bnAbs can also be characterized based on the binding conformation of the front layer region within E2 NF ('A' or 'B' conformation, Figure 5C). Taken together, structural analysis suggests that plasticity of the E2 NF can accommodate interactions with different *IGHV1-69*-encoded bnAbs that vary in CDR sequence and CDRH3 length. In this study, we extended this structural understanding to RM *VH1.36*-encoded bnAbs. Both RM2-01 and RM11-43 share overall similar characteristics with human *IGHV1-69*-encoded bnAbs (hydrophobic CDRH2 for interaction with a hydrophobic groove in E2 NF and heavy-chain dominant antigen interaction). Despite differences in CDRH3 length, the two RM bnAbs created their own subgroup, characterized by different CDR footprints; CDRH2 interacted only with the front layer, but the bAbs could also interact with back-layer residues when E2 was in the 'A' conformation. This mode of E2 binding underscored how versatile the *IGHV1-69* family and orthologs were in recognition of diverse antigenic surfaces including the flexible E2 NF. Further investigation is warranted on whether this binding mode can also be used by human *IGHV1-69*-encoded bnAbs.

With longitudinal NGS, we further characterized the BCR repertoires and *VH1.36*-encoded bnAb lineage development in the immunized RMs. The vaccine-primed B cell repertoires were predominantly enriched in B cells originated from the VH4 and VH3 families (Figures S2E and S2F), but the VH3- and VH4-derived virus-specific antibodies were mostly non-neutralizing or neutralizing with limited breadth (Figures 2A and 2B). In comparison, the *VH1.36*-derived B cells were less prevalent and underwent a rapid and transient expansion (Figures 1B and 1D and 1E). This finding may explain that, despite the induction of broad and potent *VH1.36*-encoded bnAbs (Figure 2), their serum levels were still too low to achieve broad neutralization (Chen et al., 2020).

Similar to human *IGHV1-69*-encoded bnAbs targeting the influenza HA stem (Lingwood et al., 2012; Pappas et al., 2014), the RM HCV *VH1.36*-encoded bnAbs achieved neutralization breadth through rapid lineage development with limited SHM. A S31I substitution in CDRH1 of RM2-01 and RM11-43 appeared to be sufficient to confer high affinity to autologous virus. Broader reactivity against heterologous viruses could be achieved with a few additional somatic mutations, for example, G30R in FR1, V54G in CDRH2, and R98K in CDRH3 (Figure 6). In addition, B cell precursors of several *VH1.36*-encoded bnAb lineages were identified in the naive repertoires. Key somatic mutations for affinity maturation and neutralization appeared to be present prior to immunization or accumulate shortly after immunization. Such B cell precursors or intermediates are highly desirable for bnAb development. However, the quick contraction of the *VH1.36*-derived bnAb response during this set of immunizations remains a significant concern. As vaccine-induced immunity relies on development of long-term antibody titers or serological memory, future HCV vaccine design should focus on how to improve breadth, potency, and durability of the bnAb responses. A possible approach is to display an optimized, NF-bearing E2 core multivalently on nanoparticles to achieve such bnAb responses (He et al., 2020). Such virus-like particle (VLP)-inspired vaccine solutions may warrant further investigation in the RM model.

With the failure in the clinical trial of an experimental HCV vaccine (NCT01436357) focusing on eliciting T cell responses (Cox et al., 2019), there is increasing interest in developing HCV vaccine antigens to elicit bnAbs. Hitherto, only one vaccine trial has been performed to elicit nAbs and we showed previously that RMs immunized with the same antigen produces an antibody response highly reminiscent of the human vaccination (Chen et al., 2020). The RM antibody responses target a similar set of antigenic sites with most antibodies directed to non-neutralizing or isolate-specific epitopes. Importantly, RM *VH1.36*-encoded bnAbs with similar features to human *IGHV1-69*-encoded bnAbs were isolated here, indicating that the RM model is useful for testing HCV vaccine antigens, particularly those based on ontogeny-targeting strategies, to elicit bnAbs. RMs, like humans, are ''endowed'' with a specific germline gene in their antibody repertoire that can readily target the conserved E2 NF. Detailed comparison of RM *VH1.36*-encoded and *IGHV1-69*-encoded bnAbs, and analysis of bnAb lineage development in the context of RM B cell repertoires during immunization, have therefore greatly expanded our understanding of RM as a preclinical model for HCV vaccine development.

LIMITATIONS OF THE STUDY

We determined crystal structures for only two RM *VH1.36*-encoded bnAbs, RM2-01 and RM11-43. Both antibodies were isolated from the same donor animal and engaged E2 using a binding mode that differs from that observed for human

IGHV1-69-encoded HCV bnAbs characterized so far. Further investigation is warranted as to whether this binding mode is also used by human antibodies, or whether human binding modes are also applicable to RM antibodies. Moreover, overall classification of RM Ig germline genes is at present incomplete and gene assignment can vary between databases. The lack of standardized nomenclature of RM antibody genes and incomplete reference sequences of RM Ig alleles may affect identification of authentic SHM.

STAR★METHODS

Detailed methods are provided in the online version of this paper and include the following:

- KEY RESOURCES TABLE
- RESOURCE AVAILABILITY
  - Lead contact
  - Materials availability
  - Data and code availability
- EXPERIMENTAL MODELS AND SUBJECT DETAILS
  - Rhesus macaque PBMC
- METHOD DETAILS
  - Production of monoclonal antibodies and antibody variants
  - Library preparation for NGS
  - NGS analysis
  - Expression and purification of the soluble E2 and Fabs for crystallization
  - Crystallization and structural determination of HK6a E2c3-Fab complexes
  - K_D determination
  - HCV neutralization assays
  - ELISA
  - Epitope mapping by alanine scanning mutagenesis
  - Bioinformatics
- QUANTIFICATION AND STATISTICAL ANALYSIS

SUPPLEMENTAL INFORMATION

Supplemental Information can be found online at https://doi.org/10.1016/j.immuni.2021.02.013.

ACKNOWLEDGMENTS

This work was funded in part by NIH Grants AI079031 (to M.L.), AI123861 (to M.L., J.Z., and R.L.), AI123365 and AI106005 (to M.L. and I.A.W.), Independent Research Fund Denmark (DFF-4004-00598 and DFF-8020-00391B to J.B.), Novo Nordisk Foundation (NNF17OC0029372 and NNF19OC0054518 to J.B.), Candys Foundation (to J.P., E.A., and J.B.) and Lundbeck Foundation (R303-2018-3396 to R.V.-M. and R324-2019-1375 to J.P.). Integral Molecular, Inc. is supported by U.S. Department of Health and Human Services (HHS) contract (HHSN272201400058C to B.J.D.). We thank E. Davidson for coordinating epitope mapping, X. Dai and M. Elsliger for crystallographic and computational support, and H. Tien for automated crystal screening. X-ray data sets were collected at APS beamline 23ID-B (GM/CA CAT). GM/CA@APS has been funded in whole or in part with Federal funds from the National Cancer Institute (ACB-12002) and the National Institute of General Medical Sciences (AGM-12006). This research used resources of the Advanced Photon Source, a U.S. Department of Energy (DOE) Office of Science User Facility operated for the DOE Office of Science by Argonne National Laboratory under Contract No. DE-AC02-06CH11357. This investigation used resources that were supported by Southwest National Primate Research Center (SNPRC) grant P51 OD011133 and U42OD010442 from the Office of Research Infrastructure Programs, NIH. This is manuscript #30055 from The Scripps Research Institute.

AUTHOR CONTRIBUTIONS

F.C., N.T., I.A.W., J.Z., and M.L designed and conceived the study; F.C., N.T., X.L., E.G., R.V-M., K.N., L.H., E.D., E.H.A., J.C.S. and R.S. performed experiments and analyzed data; F.C. generated mAbs, antibody variants and Fabs; N.T. determined and analyzed X-ray structures. X.L., L.H., and J.Z. performed NGS and antibodyomics analysis; F.C. performed ELISA and ELISPOT; N.T. and R.L.S. determined K_Ds; F.C., X.L., and J.Z. performed lineage tracing analysis; E.G. and K.N. performed HCVpp neutralization, antibody expression and reagents preparation; R.V.M., E.H.A., J.P. and J.B. performed HCVcc neutralization; M.H., M.E.F., A.G.I.E., and B.J.D. performed alanine scanning mutagenesis; D.C. and R.L. oversaw the nonhuman primate studies; M.L., J.Z., and I.A.W. obtained funding support; F.C., N.T., X.L., I.A.W., J.Z., and M.L. wrote the manuscript; all authors read, edited, and approved the manuscript.

DECLARATION OF INTERESTS

The authors declare no conflict of interest. M.H., M.E.F, A.G, and B.J.D. are current or former employees of Integral Molecular. B.J.D. is a shareholder of Integral Molecular.

Received: June 29, 2020
Revised: December 14, 2020
Accepted: February 10, 2021
Published: March 5, 2021

SUPPORTING CITATIONS

The following reference appears in the Supplemental Information: Keck et al., 2008, Velázquez-Moctezuma et al., 2017.

REFERENCES

Adams, P.D., Grosse-Kunstleve, R.W., Hung, L.W., Ioerger, T.R., McCoy, A.J., Moriarty, N.W., Read, R.J., Sacchettini, J.C., Sauter, N.K., and Terwilliger, T.C. (2002). PHENIX: building new software for automated crystallographic structure determination. Acta Crystallogr. D Biol. Crystallogr. *58*, 1948–1954.

Bailey, J.R., Flyak, A.I., Cohen, V.J., Li, H., Wasilewski, L.N., Snider, A.E., Wang, S., Learn, G.H., Kose, N., Loerinc, L., et al. (2017). Broadly neutralizing antibodies with few somatic mutations and hepatitis C virus clearance. JCI Insight *2*, e92872.

Bailey, J.R., Urbanowicz, R.A., Ball, J.K., Law, M., and Foung, S.K.H. (2019). Standardized method for the study of antibody neutralization of HCV pseudoparticles (HCVpp). Methods Mol. Biol. *1911*, 441–450.

Bartosch, B., Dubuisson, J., and Cosset, F.L. (2003). Infectious hepatitis C virus pseudo-particles containing functional E1-E2 envelope protein complexes. J. Exp. Med. *197*, 633–642.

Briney, B., Inderbitzin, A., Joyce, C., and Burton, D.R. (2019). Commonality despite exceptional diversity in the baseline human antibody repertoire. Nature *566*, 393–397.

Bukh, J., Meuleman, P., Tellier, R., Engle, R.E., Feinstone, S.M., Eder, G., Satterfield, W.C., Govindarajan, S., Krawczynski, K., Miller, R.H., et al. (2010). Challenge pools of hepatitis C virus genotypes 1-6 prototype strains: replication fitness and pathogenicity in chimpanzees and human liver-chimeric mouse models. J. Infect. Dis. *201*, 1381–1389.

Carlsen, T.H., Pedersen, J., Prentoe, J.C., Giang, E., Keck, Z.Y., Mikkelsen, L.S., Law, M., Foung, S.K., and Bukh, J. (2014). Breadth of neutralization and synergy of clinically relevant human monoclonal antibodies against HCV genotypes 1a, 1b, 2a, 2b, 2c, and 3a. Hepatology *60*, 1551–1562.

Chen, F., Tzarum, N., Wilson, I.A., and Law, M. (2019). V_H1-69 antiviral broadly neutralizing antibodies: genetics, structures, and relevance to rational vaccine design. Curr. Opin. Virol. *34*, 149–159.

Chen, F., Nagy, K., Chavez, D., Willis, S., McBride, R., Giang, E., Honda, A., Bukh, J., Ordoukhanian, P., Zhu, J., et al. (2020). Antibody responses to immunization with HCV envelope glycoproteins as a baseline for B-cell-based vaccine development. Gastroenterology *158*, 1058–1071.e6.

Cirelli, K.M., Carnathan, D.G., Nogal, B., Martin, J.T., Rodriguez, O.L., Upadhyay, A.A., Enemuo, C.A., Gebru, E.H., Choe, Y., Viviano, F., et al. (2019). Slow delivery immunization enhances HIV neutralizing antibody and germinal center responses via modulation of immunodominance. Cell *177*, 1153–1171.e28.

Colbert, M.D., Flyak, A.I., Ogega, C.O., Kinchen, V.J., Massaccesi, G., Hernandez, M., Davidson, E., Doranz, B.J., Cox, A.L., Crowe, J.E., Jr., and Bailey, J.R. (2019). Broadly neutralizing antibodies targeting new sites of vulnerability in hepatitis C virus E1E2. J. Virol. *93*, e02070-18.

Cox, A.L., Page, K., Melia, M., Veenhuis, R., Massaccesi, G., Osburn, W., Wagner, K., Giudice, L., Stein, E., Asher, A.K., et al. (2019). LB10. A randomized, double-blind, placebo-controlled efficacy trial of a vaccine to prevent chronic hepatitis C virus infection in an at-risk population. Open Forum Infect. Dis. *6*, S997.

Dai, K., He, L., Khan, S.N., O'Dell, S., McKee, K., Tran, K., Li, Y., Sundling, C., Morris, C.D., Mascola, J.R., et al. (2015). Rhesus macaque B-cell responses to an HIV-1 trimer vaccine revealed by unbiased longitudinal repertoire analysis. mBio *6*, e01375-15.

de Jong, Y.P., Dorner, M., Mommersteeg, M.C., Xiao, J.W., Balazs, A.B., Robbins, J.B., Winer, B.Y., Gerges, S., Vega, K., Labitt, R.N., et al. (2014). Broadly neutralizing antibodies abrogate established hepatitis C virus infection. Sci. Transl. Med. *6*, 254ra129.

DeWitt, W.S., Lindau, P., Snyder, T.M., Sherwood, A.M., Vignali, M., Carlson, C.S., Greenberg, P.D., Duerkopp, N., Emerson, R.O., and Robins, H.S. (2016). A public database of memory and naive B-cell receptor sequences. PLoS ONE *11*, e0160853.

Di Niro, R., Mesin, L., Raki, M., Zheng, N.Y., Lund-Johansen, F., Lundin, K.E., Charpilienne, A., Poncet, D., Wilson, P.C., and Sollid, L.M. (2010). Rapid generation of rotavirus-specific human monoclonal antibodies from small-intestinal mucosa. J. Immunol. *185*, 5377–5383.

Ekiert, D.C., Bhabha, G., Elsliger, M.A., Friesen, R.H., Jongeneelen, M., Throsby, M., Goudsmit, J., and Wilson, I.A. (2009). Antibody recognition of a highly conserved influenza virus epitope. Science *324*, 246–251.

Emsley, P., and Cowtan, K. (2004). Coot: model-building tools for molecular graphics. Acta Crystallogr. D Biol. Crystallogr. *60*, 2126–2132.

Flyak, A.I., Ruiz, S., Colbert, M.D., Luong, T., Crowe, J.E., Jr., Bailey, J.R., and Bjorkman, P.J. (2018). HCV broadly neutralizing antibodies use a CDRH3 disulfide motif to recognize an E2 glycoprotein site that can be targeted for vaccine design. Cell Host Microbe *24*, 703–716.e3.

Flyak, A.I., Ruiz, S.E., Salas, J., Rho, S., Bailey, J.R., and Bjorkman, P.J. (2020). An ultralong CDRH2 in HCV neutralizing antibody demonstrates structural plasticity of antibodies against E2 glycoprotein. eLife *9*, e53169.

Gao, F., Lin, X., He, L., Wang, R., Wang, H., Shi, X., Zhang, F., Yin, C., Zhang, L., Zhu, J., and Yu, L. (2019). Development of a potent and protective germline-like antibody lineage against Zika virus in a convalescent human. Front. Immunol. *10*, 2424.

Giang, E., Dorner, M., Prentoe, J.C., Dreux, M., Evans, M.J., Bukh, J., Rice, C.M., Ploss, A., Burton, D.R., and Law, M. (2012). Human broadly neutralizing antibodies to the envelope glycoprotein complex of hepatitis C virus. Proc. Natl. Acad. Sci. USA *109*, 6205–6210.

Gopal, R., Jackson, K., Tzarum, N., Kong, L., Ettenger, A., Guest, J., Pfaff, J.M., Barnes, T., Honda, A., Giang, E., et al. (2017). Probing the antigenicity of hepatitis C virus envelope glycoprotein complex by high-throughput mutagenesis. PLoS Pathog. *13*, e1006735.

Gottwein, J.M., Scheel, T.K., Jensen, T.B., Lademann, J.B., Prentoe, J.C., Knudsen, M.L., Hoegh, A.M., and Bukh, J. (2009). Development and characterization of hepatitis C virus genotype 1-7 cell culture systems: role of CD81 and scavenger receptor class B type I and effect of antiviral drugs. Hepatology *49*, 364–377.

He, L., Tzarum, N., Lin, X., Shapero, B., Sou, C., Mann, C.J., Stano, A., Zhang, L., Nagy, K., Giang, E., et al. (2020). Proof of concept for rational design of hepatitis C virus E2 core nanoparticle vaccines. Sci Adv *6*, eaaz6225, https://doi.org/10.1126/sciadv.aaz6225.

Huang, D., Abbott, R.K., Havenar-Daughton, C., Skog, P.D., Al-Kolla, R., Groschel, B., Blane, T.R., Menis, S., Tran, J.T., Thinnes, T.C., et al. (2020). B cells expressing authentic naive human VRC01-class BCRs can be recruited to germinal centers and affinity mature in multiple independent mouse models. Proc. Natl. Acad. Sci. USA *117*, 22920–22931.

Jensen, T.B., Gottwein, J.M., Scheel, T.K., Hoegh, A.M., Eugen-Olsen, J., and Bukh, J. (2008). Highly efficient JFH1-based cell-culture system for hepatitis C virus genotype 5a: failure of homologous neutralizing-antibody treatment to control infection. J. Infect. Dis. *198*, 1756–1765.

Joyce, M.G., Wheatley, A.K., Thomas, P.V., Chuang, G.Y., Soto, C., Bailer, R.T., Druz, A., Georgiev, I.S., Gillespie, R.A., Kanekiyo, M., et al.; NISC Comparative Sequencing Program (2016). Vaccine-induced antibodies that neutralize group 1 and group 2 influenza A viruses. Cell *166*, 609–623.

Keck, Z.Y., Li, T.K., Xia, J., Gal-Tanamy, M., Olson, O., Li, S.H., Patel, A.H., Ball, J.K., Lemon, S.M., and Foung, S.K. (2008). Definition of a conserved immunodominant domain on hepatitis C virus E2 glycoprotein by neutralizing human monoclonal antibodies. J. Virol. *82*, 6061–6066.

Keck, Z.Y., Wang, Y., Lau, P., Lund, G., Rangarajan, S., Fauvelle, C., Liao, G.C., Holtsberg, F.W., Warfield, K.L., Aman, M.J., et al. (2016). Affinity maturation of a broadly neutralizing human monoclonal antibody that prevents acute hepatitis C virus infection in mice. Hepatology *64*, 1922–1933.

Keck, Z.Y., Pierce, B.G., Lau, P., Lu, J., Wang, Y., Underwood, A., Bull, R.A., Prentoe, J., Velázquez-Moctezuma, R., Walker, M.R., et al. (2019). Broadly neutralizing antibodies from an individual that naturally cleared multiple hepatitis C virus infections uncover molecular determinants for E2 targeting and vaccine design. PLoS Pathog. *15*, e1007772.

Kinchen, V.J., Cox, A.L., and Bailey, J.R. (2018). Can broadly neutralizing monoclonal antibodies lead to a hepatitis C virus vaccine? Trends Microbiol. *26*, 854–864.

Kong, L., Giang, E., Nieusma, T., Kadam, R.U., Cogburn, K.E., Hua, Y., Dai, X., Stanfield, R.L., Burton, D.R., Ward, A.B., et al. (2013). Hepatitis C virus E2 envelope glycoprotein core structure. Science *342*, 1090–1094.

Kong, L., Ju, B., Chen, Y., He, L., Ren, L., Liu, J., Hong, K., Su, B., Wang, Z., Ozorowski, G., et al. (2016a). Key gp120 glycans pose roadblocks to the rapid development of VRC01-class antibodies in an HIV-1-infected Chinese donor. Immunity *44*, 939–950.

Kong, L., Lee, D.E., Kadam, R.U., Liu, T., Giang, E., Nieusma, T., Garces, F., Tzarum, N., Woods, V.L., Jr., Ward, A.B., et al. (2016b). Structural flexibility at a major conserved antibody target on hepatitis C virus E2 antigen. Proc. Natl. Acad. Sci. USA *113*, 12768–12773.

Krey, T., Meola, A., Keck, Z.Y., Damier-Piolle, L., Foung, S.K., and Rey, F.A. (2013). Structural basis of HCV neutralization by human monoclonal antibodies resistant to viral neutralization escape. PLoS Pathog. *9*, e1003364.

Lang, S., Xie, J., Zhu, X., Wu, N.C., Lerner, R.A., and Wilson, I.A. (2017). Antibody 27F3 broadly targets influenza A group 1 and 2 hemagglutinins through a further variation in IGHV1-69 antibody orientation on the HA stem. Cell Rep. *20*, 2935–2943.

Lavillette, D., Tarr, A.W., Voisset, C., Donot, P., Bartosch, B., Bain, C., Patel, A.H., Dubuisson, J., Ball, J.K., and Cosset, F.L. (2005). Characterization of host-range and cell entry properties of the major genotypes and subtypes of hepatitis C virus. Hepatology *41*, 265–274.

Law, M., Maruyama, T., Lewis, J., Giang, E., Tarr, A.W., Stamataki, Z., Gastaminza, P., Chisari, F.V., Jones, I.M., Fox, R.I., et al. (2008). Broadly neutralizing antibodies protect against hepatitis C virus quasispecies challenge. Nat. Med. *14*, 25–27.

Li, Y.-P., Ramirez, S., Mikkelsen, L., and Bukh, J. (2015). Efficient infectious cell culture systems of the hepatitis C virus (HCV) prototype strains HCV-1 and H77. J. Virol. *89*, 811–823.

Lingwood, D., McTamney, P.M., Yassine, H.M., Whittle, J.R., Guo, X., Boyington, J.C., Wei, C.J., and Nabel, G.J. (2012). Structural and genetic basis for development of broadly neutralizing influenza antibodies. Nature *489*, 566–570.

Major, M., and Law, M. (2019). Detection of antibodies to HCV E1E2 by lectin-capture ELISA. Methods Mol. Biol. *1911*, 421–432.

McCoy, A.J., Grosse-Kunstleve, R.W., Storoni, L.C., and Read, R.J. (2005). Likelihood-enhanced fast translation functions. Acta Crystallogr. D Biol. Crystallogr. *61*, 458–464.

Merat, S.J., Molenkamp, R., Wagner, K., Koekkoek, S.M., van de Berg, D., Yasuda, E., Böhne, M., Claassen, Y.B., Grady, B.P., Prins, M., et al. (2016). Hepatitis C virus broadly neutralizing monoclonal antibodies isolated 25 years after spontaneous clearance. PLoS ONE *11*, e0165047.

Merat, S.J., Bru, C., van de Berg, D., Molenkamp, R., Tarr, A.W., Koekkoek, S., Kootstra, N.A., Prins, M., Ball, J.K., Bakker, A.Q., et al. (2019). Cross-genotype AR3-specific neutralizing antibodies confer long-term protection in injecting drug users after HCV clearance. J. Hepatol. *71*, 14–24.

Meunier, J.-C., Engle, R.E., Faulk, K., Zhao, M., Bartosch, B., Alter, H., Emerson, S.U., Cosset, F.-L., Purcell, R.H., and Bukh, J. (2005). Evidence for cross-genotype neutralization of hepatitis C virus pseudo-particles and enhancement of infectivity by apolipoprotein C1. Proc. Natl. Acad. Sci. USA *102*, 4560–4565.

Otwinowski, Z., and Minor, W. (1997). Processing of X-ray diffraction data collected in oscillation mode. Methods Enzymol. *276*, 307–326.

Pappas, L., Foglierini, M., Piccoli, L., Kallewaard, N.L., Turrini, F., Silacci, C., Fernandez-Rodriguez, B., Agatic, G., Giacchetto-Sasselli, I., Pellicciotta, G., et al. (2014). Rapid development of broadly influenza neutralizing antibodies through redundant mutations. Nature *516*, 418–422.

Pedersen, J., Carlsen, T.H., Prentoe, J., Ramirez, S., Jensen, T.B., Forns, X., Alter, H., Foung, S.K., Law, M., Gottwein, J., et al. (2013). Neutralization resistance of hepatitis C virus can be overcome by recombinant human monoclonal antibodies. Hepatology *58*, 1587–1597.

Prentoe, J., and Bukh, J. (2019). In vitro neutralization assay using cultured hepatitis C virus. Methods Mol. Biol. *1911*, 433–439.

Prentoe, J., Jensen, T.B., Meuleman, P., Serre, S.B., Scheel, T.K., Leroux-Roels, G., Gottwein, J.M., and Bukh, J. (2011). Hypervariable region 1 differentially impacts viability of hepatitis C virus strains of genotypes 1 to 6 and impairs virus neutralization. J. Virol. *85*, 2224–2234.

Ramesh, A., Darko, S., Hua, A., Overman, G., Ransier, A., Francica, J.R., Trama, A., Tomaras, G.D., Haynes, B.F., Douek, D.C., and Kepler, T.B. (2017). Structure and diversity of the rhesus macaque immunoglobulin loci through multiple *de novo* genome assemblies. Front. Immunol. *8*, 1407.

Robbiani, D.F., Gaebler, C., Muecksch, F., Lorenzi, J.C.C., Wang, Z., Cho, A., Agudelo, M., Barnes, C.O., Gazumyan, A., Finkin, S., et al. (2020). Convergent antibody responses to SARS-CoV-2 in convalescent individuals. Nature *584*, 437–442.

Roccasecca, R., Ansuini, H., Vitelli, A., Meola, A., Scarselli, E., Acali, S., Pezzanera, M., Ercole, B.B., McKeating, J., Yagnik, A., et al. (2003). Binding of the hepatitis C virus E2 glycoprotein to CD81 is strain specific and is modulated by a complex interplay between hypervariable regions 1 and 2. J. Virol. *77*, 1856–1867.

Sangesland, M., Ronsard, L., Kazer, S.W., Bals, J., Boyoglu-Barnum, S., Yousif, A.S., Barnes, R., Feldman, J., Quirindongo-Crespo, M., McTamney, P.M., et al. (2019). Germline-encoded affinity for cognate antigen enables vaccine amplification of a human broadly neutralizing response against influenza virus. Immunity *51*, 735–749.e8.

Scheel, T.K.H., Gottwein, J.M., Carlsen, T.H.R., Li, Y.-P., Jensen, T.B., Spengler, U., Weis, N., and Bukh, J. (2011). Efficient culture adaptation of hepatitis C virus recombinants with genotype-specific core-NS2 by using previously identified mutations. J. Virol. *85*, 2891–2906.

Scheel, T.K.H., Gottwein, J.M., Jensen, T.B., Prentoe, J., Hoegh, A.M., Alter, H.J., Eugen-Olsen, J., and Bukh, J. (2008). Development of JFH1-based cell culture systems for hepatitis C virus genotype 4a and evidence for cross-genotype neutralization. Proc. Natl. Acad. Sci. USA *105*, 997–1002.

Sundling, C., Li, Y., Huynh, N., Poulsen, C., Wilson, R., O'Dell, S., Feng, Y., Mascola, J.R., Wyatt, R.T., and Karlsson Hedestam, G.B. (2012a). High-resolution definition of vaccine-elicited B cell responses against the HIV primary receptor binding site. Sci. Transl. Med. *4*, 142ra96.

Sundling, C., Phad, G., Douagi, I., Navis, M., and Karlsson Hedestam, G.B. (2012b). Isolation of antibody V(D)J sequences from single cell sorted rhesus macaque B cells. J. Immunol. Methods *386*, 85–93.

Tian, M., Cheng, C., Chen, X., Duan, H., Cheng, H.L., Dao, M., Sheng, Z., Kimble, M., Wang, L., Lin, S., et al. (2016). Induction of HIV neutralizing antibody lineages in mice with diverse precursor repertoires. Cell *166*, 1471–1484.e18.

Tiller, T., Meffre, E., Yurasov, S., Tsuiji, M., Nussenzweig, M.C., and Wardemann, H. (2008). Efficient generation of monoclonal antibodies from single human B cells by single cell RT-PCR and expression vector cloning. J. Immunol. Methods *329*, 112–124.

Tzarum, N., Giang, E., Kadam, R.U., Chen, F., Nagy, K., Augestad, E.H., Velázquez-Moctezuma, R., Keck, Z.Y., Hua, Y., Stanfield, R.L., et al. (2020). An alternate conformation of HCV E2 neutralizing face as a new vaccine target. Sci Adv *6*, eabb5642, https://doi.org/10.1126/sciadv.abb5642.

Tzarum, N., Giang, E., Kong, L., He, L., Prentoe, J., Augestad, E., Hua, Y., Castillo, S., Lauer, G.M., Bukh, J., et al. (2019). Genetic and structural insights into broad neutralization of hepatitis C virus by human IGHV1-69 antibodies. Sci Adv *5*, eaav1882, https://doi.org/10.1126/sciadv.aav1882.

Tzarum, N., Wilson, I.A., and Law, M. (2018). The neutralizing face of hepatitis C virus E2 envelope glycoprotein. Front. Immunol. *9*, 1315.

Umotoy, J., Bagaya, B.S., Joyce, C., Schiffner, T., Menis, S., Saye-Francisco, K.L., Biddle, T., Mohan, S., Vollbrecht, T., Kalyuzhniy, O., et al.; IAVI Protocol C Investigators; IAVI African HIV Research Network (2019). Rapid and focused maturation of a VRC01-class HIV broadly neutralizing antibody lineage involves both binding and accommodation of the N276-glycan. Immunity *51*, 141–154.e6.

Velázquez-Moctezuma, R., Law, M., Bukh, J., and Prentoe, J. (2017). Applying antibody-sensitive hypervariable region 1-deleted hepatitis C virus to the study of escape pathways of neutralizing human monoclonal antibody AR5A. PLoS Pathog. *13*, e1006214.

Velázquez-Moctezuma, R., Galli, A., Law, M., Bukh, J., and Prentoe, J. (2019). Hepatitis C virus escape studies of human antibody AR3A reveal a high barrier to resistance and novel insights on viral antibody evasion mechanisms. J. Virol. *93*, e01909–e01918.

Vigdorovich, V., Oliver, B.G., Carbonetti, S., Dambrauskas, N., Lange, M.D., Yacoob, C., Leahy, W., Callahan, J., Stamatatos, L., and Sather, D.N. (2016). Repertoire comparison of the B-cell receptor-encoding loci in humans and rhesus macaques by next-generation sequencing. Clin. Transl. Immunology *5*, e93.

Weitkamp, J.H., Kallewaard, N.L., Bowen, A.L., Lafleur, B.J., Greenberg, H.B., and Crowe, J.E., Jr. (2005). VH1-46 is the dominant immunoglobulin heavy chain gene segment in rotavirus-specific memory B cells expressing the intestinal homing receptor $\alpha_4\beta_7$. J. Immunol. *174*, 3454–3460.

Wen, G.P., He, L., Tang, Z.M., Wang, S.L., Zhang, X., Chen, Y.Z., Lin, X., Liu, C., Chen, J.X., Ying, D., et al. (2020). Quantitative evaluation of protective antibody response induced by hepatitis E vaccine in humans. Nat. Commun. *11*, 3971.

Wheatley, A.K., Whittle, J.R., Lingwood, D., Kanekiyo, M., Yassine, H.M., Ma, S.S., Narpala, S.R., Prabhakaran, M.S., Matus-Nicodemos, R.A., Bailer, R.T., et al. (2015). H5N1 vaccine-elicited memory B cells are genetically constrained by the IGHV locus in the recognition of a neutralizing epitope in the hemagglutinin stem. J. Immunol. *195*, 602–610.

Wu, X., Zhou, T., Zhu, J., Zhang, B., Georgiev, I., Wang, C., Chen, X., Longo, N.S., Louder, M., McKee, K., et al.; NISC Comparative Sequencing Program (2011). Focused evolution of HIV-1 neutralizing antibodies revealed by structures and deep sequencing. Science *333*, 1593–1602.

Wu, X., Zhang, Z., Schramm, C.A., Joyce, M.G., Kwon, Y.D., Zhou, T., Sheng, Z., Zhang, B., O'Dell, S., McKee, K., et al.; NISC Comparative Sequencing Program (2015). Maturation and diversity of the VRC01-antibody lineage over 15 years of chronic HIV-1 infection. Cell *161*, 470–485.

Ye, J., Ma, N., Madden, T.L., and Ostell, J.M. (2013). IgBLAST: an immunoglobulin variable domain sequence analysis tool. Nucleic Acids Res. *41*, W34–W40.

Yuan, M., Liu, H., Wu, N.C., Lee, C.D., Zhu, X., Zhao, F., Huang, D., Yu, W., Hua, Y., Tien, H., et al. (2020). Structural basis of a shared antibody response to SARS-CoV-2. Science *369*, 1119–1123.

Zhou, T., Lynch, R.M., Chen, L., Acharya, P., Wu, X., Doria-Rose, N.A., Joyce, M.G., Lingwood, D., Soto, C., Bailer, R.T., et al.; NISC Comparative Sequencing Program (2015). Structural repertoire of HIV-1-neutralizing antibodies targeting the CD4 supersite in 14 donors. Cell *161*, 1280–1292.

Please cite this article in press as: Chen et al., Functional convergence of a germline-encoded neutralizing antibody response in rhesus macaques immunized with HCV envelope glycoproteins, Immunity (2021), https://doi.org/10.1016/j.immuni.2021.02.013

STAR★METHODS

KEY RESOURCES TABLE

REAGENT or RESOURCE	SOURCE	IDENTIFIER
Antibodies		
PE/Cy7 anti-human CD3 (clone SP34-2)	BD Biosciences	Cat#557749
PerCP/Cy5.5 anti-human CD20 (clone 2H7)	BioLegend	Cat#302326; RRID: AB_893283
APC anti-human CD20 (clone 2H7)	BioLegend	Cat#302310; RRID: AB_314258
PE/Cy5 anti-human CD80 (clone L307.4)	BD Biosciences	Cat#559370
BV421 anti-human HLA-DR (clone L243)	BioLegend	Cat#307636; RRID: AB_2561831
PE anti-human CD27 (clone O323)	BioLegend	Cat#302808; RRID: AB_314300
FITC anti-human IgG (clone G18-145)	BD Biosciences	Cat#555786
HRP-conjugated goat anti-human IgG Fc	Jackson ImmunoResearch	Cat# 109-035-008; RRID: AB_2337579
AR3A	(Giang et al., 2012)	N/A
HEPC74	Bailey et al., 2017	N/A
HC84.1	Krey et al., 2013	N/A
212.1.1	Keck et al., 2019	N/A
RM2-01	Chen et al., 2020	N/A
RM11-43	Chen et al., 2020	N/A
Bacterial and Virus Strains		
JFH1-based HCV recombinant with Core-NS2 of H77	Li et al., 2015; Carlsen et al., 2014	N/A
JFH1-based HCV recombinant with Core-NS2 of H77ΔHVR1	Prentoe et al., 2011	N/A
JFH1-based HCV recombinant with Core-NS2 of TN	Carlsen et al., 2014	N/A
JFH1-based HCV recombinant with Core-NS2 of DH1	Carlsen et al., 2014	N/A
JFH1-based HCV recombinant with Core-NS2 of J4	Carlsen et al., 2014	N/A
JFH1-based HCV recombinant with Core-NS2 of J6	Carlsen et al., 2014	N/A
JFH1-based HCV recombinant with Core-NS2 of J8	Carlsen et al., 2014	N/A
JFH1-based HCV recombinant with Core-NS2 of S52	Carlsen et al., 2014	N/A
JFH1-based HCV recombinant with Core-NS2 of DBN	Carlsen et al., 2014	N/A
JFH1-based HCV recombinant with Core-NS2 of ED43	(Scheel et al., 2008)	N/A
JFH1-based HCV recombinant with Core-NS2 of SA13	Jensen et al., 2008	N/A
JFH1-based HCV recombinant with Core-NS2 of HK6a	(Gottwein et al., 2009)	N/A
Biological Samples		
PBMC samples from rhesus macaques	Chen et al., 2020	N/A
Chemicals, Peptides, and Recombinant Proteins		
HCV-1 E2ΔTM	Chen et al., 2020	N/A
HK6a E2c3	Tzarum et al., 2019	N/A
Critical Commercial Assays		
Alexa Fluor™ 647 Protein Labeling Kit	Thermo Fisher Scientific	Cat#A20173
ExpiFectamine CHO Transfection Kit	Thermo Fisher Scientific	Cat#A29127
Deposited Data		
HK6a E2c3-RM2-01 structure	This paper	PDB: 7JTF
HK6a E2c3-RM11-43 structure	This paper	PDB: 7JTG
Experimental Models: Cell Lines		
ExpiCHO-S cells	Thermo Fisher Scientific	Cat#A29127; RRID: CVCL_5J31
Huh 7 cells	APATH	N/A

(*Continued on next page*)

Please cite this article in press as: Chen et al., Functional convergence of a germline-encoded neutralizing antibody response in rhesus macaques immunized with HCV envelope glycoproteins, Immunity (2021), https://doi.org/10.1016/j.immuni.2021.02.013

Continued

REAGENT or RESOURCE	SOURCE	IDENTIFIER
Huh 7.5 cells	APATH	N/A
HEK293T cells	ATCC	Cat# CRL-3216; RRID:CVCL_0063
Oligonucleotides		
Primers for mAb cloning	Sundling et al., 2012b	N/A
Primers for NGS library	Dai et al., 2015	N/A
Recombinant DNA		
Human Igγ1 expression vector	Tiller et al., 2008	N/A
Human Igκ expression vector	Tiller et al., 2008	N/A
Human Igλ expression vector	Tiller et al., 2008	N/A
HCV-1 E1E2 expression vector	Li et al., 2015	N/A
H77 E1E2 expression vector	Meunier et al., 2005	N/A
UKN1B 12.6 E1E2 expression vector	Lavillette et al., 2005	N/A
J6 E1E2 expression vector	Meunier et al., 2005	N/A
S52 E1E2 expression vector	Meunier et al., 2005	N/A
UKN4.11.1 E1E2 expression vector	Lavillette et al., 2005	N/A
SA13 E1E2 expression vector	Meunier et al., 2005	N/A
HK6a E1E2 expression vector	Meunier et al., 2005	N/A
Software and Algorithms		
Prism 9	GraphPad	https://www.graphpad.com/scientific-software/prism/; RRID: SCR_002798
Lasergene 17	DNAstar	https://www.dnastar.com/software/lasergene/; RRID:SCR_000291
MEGA X	MEGA	https://www.megasoftware.net/; RRID:SCR_000667
IgBLAST	NCBI	https://www.ncbi.nlm.nih.gov/projects/igblast/; RRID:SCR_002873
abYsis	abYsis	http://www.abysis.org/abysis/; RRID:SCR_000756
IMGT/V-QUEST	IMGT	http://www.imgt.org/; RRID: SCR_012780
PyMOL	Schrodinger LLC	https://www.schrodinger.com/pymol; RRID: SCR_000305

RESOURCE AVAILABILITY

Lead contact

Further information and requests for resources and reagent should be directed to and will be fulfilled by the lead contact, Mansun Law, D.Phil. (mlaw@scripps.edu).

Materials availability

Antibodies generated in this study are available from the Lead Contact with a completed Materials Transfer Agreement.

Data and code availability

The accession numbers for HK6a E2c3-RM2-01 and HK6a E2c3-RM11-43 structures reported in this paper are PDB: 7JTF and 7JTG, respectively.

EXPERIMENTAL MODELS AND SUBJECT DETAILS

Rhesus macaque PBMC

PBMC samples from rhesus macaques (#30734, #31881, #31782 and #31859) were collected from a previous HCV Env immunization study (Chen et al., 2020). All procedures and experiments in RMs were performed in accordance with protocols reviewed and approved by the Institutional Animal Care and Use Committees (IACUC) of TBRI and The Scripps Research Institute (TSRI).

Please cite this article in press as: Chen et al., Functional convergence of a germline-encoded neutralizing antibody response in rhesus macaques immunized with HCV envelope glycoproteins, Immunity (2021), https://doi.org/10.1016/j.immuni.2021.02.013

METHOD DETAILS

Production of monoclonal antibodies and antibody variants

Monoclonal antibodies (mAbs) were generated from single plasmablasts ($CD3^-CD20^-CD80^+HLA\text{-}DR^+$) and E2-specific memory B cells ($CD3^-CD20^+CD27^+IgG^+$ $E2^+$) of animals #30734 and #31881 as previously described (Chen et al., 2020). The Ig heavy-chain and light-chain variable genes from single plasmablasts and E2-specific memory B cells were amplified (Sundling et al., 2012b) and cloned into human Igγ1, Igκ and Igλ expression vectors (Tiller et al., 2008). The heavy-chain variants and NGS identified heavy chains were produced by GeneArt gene synthesis (Thermo Fisher Scientific) or Q5 site-directed mutagenesis kit (NEB). Plasmids containing paired antibody heavy- and light-chain genes were co-transfected (1:1 ratio) into ExpiCHO cells using ExpiFectamine CHO Transfection Kit (Thermo Fisher Scientific). Antibody-containing supernatants were harvested 14 days after transfection, filtered through 0.22 μm filters and purified over Protein A-Sepharose 4 Fast Flow (GE healthcare) column per manufacturer's instruction.

Library preparation for NGS

The dynamics of global B cell repertoires of animals #30734 and #31881 were analyzed by longitudinal NGS of the full-length antibody variable domains of total B cells from PMBCs collected at indicated time points (Figure 1A). For antigen-specific B cell repertoire analysis, E2-specific memory B cells were bulk sorted from PBMCs of animals #31782 and #31859 collected at day 10 after the 4^{th} immunization. A 5'-rapid amplification of cDNA ends (RACE) protocol previously reported for unbiased sequencing of RM B cell repertoires (Dai et al., 2015; Wen et al., 2020) was applied. Briefly, total RNA was extracted from 1:5 million PBMCs into 30 μL of water with RNeasy Mini Kits (QIAGEN). 5'-RACE was performed with SMARTer RACE cDNA Amplification Kit (Clontech). The cDNA was purified and eluted in 20 μL of elution buffer (NucleoSpin PCR Clean-up Kit, Clontech). The Ig PCRs were set up with Platinum Taq High- Fidelity DNA Polymerase (Life Technologies) in a total volume of 50 μl, with 5 μL of cDNA as template, 1 μL of 5'-RACE primer, and 1 μL of 10 μM reverse primer. To facilitate deep sequencing on the Ion GeneStudio S5 system, the forward primers contained a P1 adaptor, while the reverse primer contained an A adaptor and an Ion XpressTM barcode (Life Technologies) to differentiate the libraries from various time points. A total of 25 cycles of PCRs were performed and the PCR products (:620 bp) were gel purified (QIAGEN).

NGS analysis

NGS was performed on the Ion S5 GeneStudio system. Briefly, heavy-chain libraries from different time points were quantitated using Qubit® 2.0 Fluorometer with Qubit® dsDNA HS Assay Kit, and then mixed at an equal ratio for sequencing. Template preparation and (Ion 530) chip loading were performed on Ion Chef using the Ion 520/530 Ext Kit, followed by sequencing on the Ion S5 system with default settings. An improved version of the *Antibodyomics* pipeline (Wen et al., 2020) was adapted for RM library and used to process the raw data and determine distributions for germline gene usage, somatic hypermutation, germline divergence, and CDRH3 loop length. The two-dimensional (2D) identity-divergence plots were constructed to visualize specific antibody lineages in the context of antibody repertoire at each time point. CDR3 identity of 95% was used as the cutoff for identifying sequences evolutionarily related to a reference antibody (shown as magenta dots on the 2D plots). A consensus or a manually selected sequence was used for antibody synthesis and functional characterization.

Expression and purification of the soluble E2 and Fabs for crystallization

The E2 constructs were expressed and proteins were purified as previously described (Tzarum et al., 2019). The heavy-chain and light-chain sequences of RM2-01 and RM11-43 Fab fragments were generated and expressed in ExpiCHO cells. The mAbs were purified on a protein G affinity column followed by size exclusion chromatography using a Superdex-200 column (GE Healthcare) in 50 mM NaCl, 20 mM Tris-HCl (pH 7.2) buffer.

Crystallization and structural determination of HK6a E2c3-Fab complexes

The E2-Fab complexes were formed by overnight incubation of purified E2 and Fabs in a molar ratio of 1:1.25 (E2:Fab) at room temperature followed by size exclusion chromatography (Superdex-200) to remove unbound Fabs using 20 mM Tris and 50 mM NaCl (pH 7.2) buffer. Crystallization experiments were performed using the vapor diffusion sitting drop method at 20°C. Crystals of HK6a E2c3-RM2-01 and HK6a E2c3-RM11-43 diffracted to 3.35 Å and 2.60 Å, respectively (Table S2). Crystals of the E2c3 HK6a-RM2-01 complex were obtained using a reservoir solution of 30% PEG 400, 0.1M Cd chloride, 0.1M sodium acetate, pH 4.6, and crystals of E2c3 HK6a-RM11-43 complex from 20% (w/v) PEG 3350, 0.2M sodium sulfate, pH 6.6. Prior to data collection, E2c3 HK6a-RM11-43 crystals were cryoprotected with 10% ethylene glycol (no additional cryoprotectant was required for E2c3 HK6a-RM2-01 crystals) and flash cooled in liquid nitrogen. Diffraction datasets were collected at the Advanced Photon Source (APS, Table S2). Data were integrated and scaled using HKL-2000 (Otwinowski and Minor, 1997). The E2c3-Fab structures were solved by molecular replacement using Phaser (McCoy et al., 2005) with E2c3 HK6a-AR3A (PDB: 6BKB) as the search model. Structure refinement was carried out in Phenix (Adams et al., 2002) and model building with COOT (Emsley and Cowtan, 2004). Final refinement statistics are summarized in Table S2.

Please cite this article in press as: Chen et al., Functional convergence of a germline-encoded neutralizing antibody response in rhesus macaques immunized with HCV envelope glycoproteins, Immunity (2021), https://doi.org/10.1016/j.immuni.2021.02.013

K_D determination

K_D values were determined by bio-layer interferometry (BLI) using an Octet RED instrument (ForteBio, Inc.). IgGs at ~10 μg /mL in a kinetics buffer (1 × PBS, 0.01% BSA and 0.002% Tween 20, pH 7.4) were immobilized onto protein G-coated biosensors. A two-fold concentration gradient of E2, starting at 10μM, 20μM or 40μM depending on the binding affinity, was used in a titration series of five. The k_{on} and k_{off} values of E2 protein for each IgG were measured in real time to determine K_D values. All binding data were collected at 30 °C.

HCV neutralization assays

HCV pseudoparticles (HCVpp) were generated by co-transfection of 293T cells with pNL4-3.lucR$^-$E$^-$ and the corresponding expression plasmids encoding the E1E2 from isolate HCV-1, H77, UKN1B 12.6, J6, S52, UKN4.11.1 or SA13 (Bartosch et al., 2003; Lavillette et al., 2005; Li et al., 2015; Meunier et al., 2005) at a 4:1 ratio by polyethylenimine (PEI, Polysciences). HCVpp neutralization was carried out on Huh 7 cells with mAbs (50 μg/mL) as previously described (Bailey et al., 2019). Virus infectivity was detected with Bright-Glo luciferase assay system (Promega), and percent neutralization was calculated as the virus infectivity inhibited at the antibody concentrations divided by the infectivity without antibody after background subtraction. The background infectivity of the pseudotype virus was defined by infecting cells with virus made only with pNL4-3.lucR-E-. Pseudoparticles displaying the vesicular stomatitis virus envelope glycoprotein G (VSVpp) were used as a control for nonspecific neutralizing activity.

For HCV cell culture (HCVcc) neutralization, HCV isolates H77, H77ΔHVR1, TN, DH1, J4, J6, J8, S52, DBN, ED43, SA13 and HK6a (Carlsen et al., 2014; Gottwein et al., 2009; Jensen et al., 2008; Li et al., 2015; Pedersen et al., 2013; Prentoe et al., 2011; Scheel et al., 2011) were propagated in Huh 7.5 cells. Neutralization was performed as previously described (Prentoe and Bukh, 2019). Briefly, viruses were preincubated with mAb (at 50 μg/mL or a dilution series) for 1 h at 37°C and then added to Huh7.5 cells plated at 7×10^3 in poly-D-lysine-coated 96-well plates the day before. After 4 h incubation with the virus/antibody mix, the cells were washed and incubated in fresh medium for a total infection time of 48 h. Cells were then fixed and stained with 9E10 antibody. The data were normalized with 8 replicates of virus only and analyzed using GraphPad Prism.

ELISA

Methods for measuring anti-E1E2 antibody titers have been described elsewhere (Major and Law, 2019). Briefly, Costar High Binding Half-Area 96-well plates (Corning) were coated overnight at 4°C with 5 μg/mL of *G. nivalis* lectin (GNL, Vector Laboratories). After blocking with 4% nonfat milk (Bio-Rad) in PBS + 0.05% Tween-20 (PBS-T), plates were incubated with batch-diluted cell lysates from 293T cells expressing E1E2 at room temperature for 1 h. Serial dilutions of antibodies were then added and incubated at room temperature for at least 1 h. Horseradish peroxidase (HRP)-conjugated goat anti-human IgG Fc antibody (1:2,000, Jackson ImmunoResearch) was used for detection.

Epitope mapping by alanine scanning mutagenesis

High-throughput scanning mutagenesis using an HCV E1E2 alanine scanning library (genotype 1a, strain H77; GenBank:: NC_004102) was performed as described previously (Gopal et al., 2017). Binding of the mAb to an individual alanine mutant was expressed as percentage of the mAb binding signal obtained with wild type E1E2.

Bioinformatics

Antibody sequences were submitted to IgBLAST (https://www.ncbi.nlm.nih.gov/igblast/) and ImMunoGeneTics information system (IMGT, http://www.imgt.org/) for gene identification and genetic assignment. Multiple-sequence alignments were performed using MegAlign Pro program in Lasergene 17 (DNAstar). Maximum-likelihood phylogenetic tree was constructed using MEGA X software.

QUANTIFICATION AND STATISTICAL ANALYSIS

Graphpad Prism v9 was used for all statistical analyses. The significance of differences in CDRH3 length and SHM between RM and human antibodies was calculated using unpaired, two-tailed Mann-Whitney U tests. Data were considered statistically significant at $^*p < 0.05$, $^{**}p < 0.001$, $^{***}p < 0.0001$.